AD_____

GRANT NUMBER DAMD17-94-J-4117

TITLE: Role of Accessory Molecule(s) in Endotoxin-Endothelial Interactions and Endothelial Barrier Dysfunction

PRINCIPAL INVESTIGATOR: Simeon E. Goldblum, M.D.

CONTRACTING ORGANIZATION: University of Maryland
School of Medicine
Baltimore, Maryland 21201

REPORT DATE: July 1996

TYPE OF REPORT: Annual

PREPARED FOR: Commander
U.S. Army Medical Research and Materiel Command
Fort Detrick, Frederick, Maryland 21702-5012

REPORT DOCUMENTATION PAGE

Form Approved
OMB No. 0704-0188

1. AGENCY USE ONLY *(Leave blank)*	2. REPORT DATE	3. REPORT TYPE AND DATES COVERED
	July 1996	Annual (1 Jun 95 - 31 May 96)

4. TITLE AND SUBTITLE Role of Accessory Molecule(s) in Endotoxin-Endothelial Interactions and Endothelial Barrier Dysfunction

5. FUNDING NUMBERS
DAMD17-94-J-4117

6. AUTHOR(S)
Simeon E. Goldblum, M.D.

7. PERFORMING ORGANIZATION NAME(S) AND ADDRESS(ES)
University of Maryland School of Medicine
Baltimore, Maryland 21201

8. PERFORMING ORGANIZATION REPORT NUMBER

9. SPONSORING/MONITORING AGENCY NAME(S) AND ADDRESS(ES)
Commander
U.S. Army Medical Research and Materiel Command
Fort Detrick, MD 21702-5012

10. SPONSORING/MONITORING AGENCY REPORT NUMBER

11. SUPPLEMENTARY NOTES

12a. DISTRIBUTION / AVAILABILITY STATEMENT
Approved for public release; distribution unlimited

12b. DISTRIBUTION CODE

13. ABSTRACT *(Maximum 200*

This grant has been renegotiated and the new technical objectives are:

1) To determine whether LPS induces tyrosine phosphorylation of endothelial cell proteins that can be coupled to changes in barrier function.

2) To determine whether this LPS-induced endothelial intercellular gap formation and barrier dysfunction is due to zonula adherens and/or focal adhesion disassembly.

3) To determine which protein substrates are the targets of LPS-induced tyrosine phosphorylation.

14. SUBJECT TERMS
endothelium, barrier function, endotoxin, tyrosine phosphorylation, actin cytoskeleton

15. NUMBER OF PAGES
53

16. PRICE CODE

17. SECURITY CLASSIFICATION OF REPORT	18. SECURITY CLASSIFICATION OF THIS PAGE	19. SECURITY CLASSIFICATION OF ABSTRACT	20. LIMITATION OF ABSTRACT
Unclassified	Unclassified	Unclassified	Unlimited

DISCLAIMER NOTICE

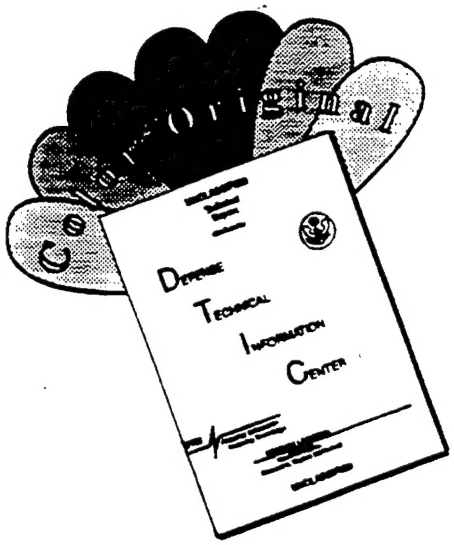

THIS DOCUMENT IS BEST QUALITY AVAILABLE. THE COPY FURNISHED TO DTIC CONTAINED A SIGNIFICANT NUMBER OF COLOR PAGES WHICH DO NOT REPRODUCE LEGIBLY ON BLACK AND WHITE MICROFICHE.

FOREWORD

Opinions, interpretations, conclusions and recommendations are those of the author and are not necessarily endorsed by the US Army.

SEG Where copyrighted material is quoted, permission has been obtained to use such material.

____ Where material from documents designated for limited distribution is quoted, permission has been obtained to use the material.

SEG Citations of commercial organizations and trade names in this report do not constitute an official Department of Army endorsement or approval of the products or services of these organizations.

____ In conducting research using animals, the investigator(s) adhered to the "Guide for the Care and Use of Laboratory Animals," prepared by the Committee on Care and Use of Laboratory Animals of the Institute of Laboratory Resources, National Research Council (NIH Publication No. 86-23, Revised 1985).

____ For the protection of human subjects, the investigator(s) adhered to policies of applicable Federal Law 45 CFR 46.

____ In conducting research utilizing recombinant DNA technology, the investigator(s) adhered to current guidelines promulgated by the National Institutes of Health.

____ In the conduct of research utilizing recombinant DNA, the investigator(s) adhered to the NIH Guidelines for Research Involving Recombinant DNA Molecules.

SEG In the conduct of research involving hazardous organisms, the investigator(s) adhered to the CDC-NIH Guide for Biosafety in Microbiological and Biomedical Laboratories.

Simeon E Goldman 8/2/96

PI - Signature Date

(4) TABLE OF CONTENTS

INTRODUCTION

The frequency of Gram-negative bacteremia and its associated mortality continues to increase despite the advent of improved antibiotic therapy. Complications resulting from these infections include: profound shock, disseminated intravascular coagulation, and the development of vascular leak syndromes, the most notable of which is acute respiratory distress syndrome (1-3). A common denominator to all of these complications is endothelial cell (EC) injury. Bacterial endotoxin or lipopolysaccharide (LPS), a component of the envelope of Gram-negative organisms, has been shown to directly provoke the EC injury associated with Gram-negative sepsis (4). Data exists to support LPS as a key mediator of EC injury including: 1) LPS plasma levels correlate with the development of septic shock and multiorgan failure (5), 2) administration of LPS alone to experimental animals reproduces the EC injury seen in animals challenged with Gram-negative bacteria (4), and 3) interventions which specifically target the LPS molecule protect against the EC complications often associated with Gram-negative sepsis (6-8).

LPS directly induces pulmonary vascular EC injury *in vitro* in the absence of nonendothelial-derived host mediators (9). EC responses to LPS include: F-actin depolymerization and microfilament redistribution, changes in cell morphology, intercellular gap formation, and increased monolayer permeability (10,11).

The state of assembly and organization of the actin cytoskeletal network is closely linked to changes in EC monolayer permeability (12-14). Adherens junctions, which are responsible for cell-cell (zonula adherens) and cell-substrate (focal adhesions) adhesion and which are coupled to the actin cytoskeleton, play a key role in maintaining the integrity of EC monolayers. It has been suggested that an increased state of protein tyrosine phosphorylation may lead to cytoskeletal reorganization and changes in cellular junctions which compromise monolayer integrity (14,15).

The presentation of LPS to CD14 bearing cells such as macrophages and monocytes has been well characterized. LPS binds with the acute phase protein lipopolysaccharide binding protein and the resulting complex recognizes membrane bound CD14 (16). CD14, a glycosylphosphatidyl inositol-anchored protein, has not been demonstrated to play a primary role in signal transduction, yet rapid tyrosine phosphorylation occurs after binding of LPS to CD14 (16). Even less is known about the interactions of LPS with non-CD14 bearing cells including EC. Recently, tyrosine phosphorylation of mitogen-activated protein kinases has been demonstrated in LPS-stimulated EC (17). Furthermore, PTK inhibition has been shown to attenuate LPS-induced EC toxicity (18) and interleukin-6 (IL-6) release *in vitro* (20), and to prevent LPS-induced lethality in mice (19).

We now report that LPS induces tyrosine phosphorylation of a 65 kDa protein, identified as paxillin, in bovine pulmonary vascular EC. Further, we have demonstrated

that LPS-induced actin depolymerization, intercellular gap formation, and disruption of endothelial barrier function are mediated through protein tyrosine phosphorylation. Finally, we have demonstrated that the recombinant form of a protein derived from *Limulus polyphemus*, endotoxin neutralizing protein (ENP) (20-24), can block LPS-induced tyrosine phosphorylation of EC proteins, actin depolymerization, opening of the paracellular pathway, and loss of barrier function.

METHODS AND MATERIALS

LPS Preparations:

LPS phenol-extracted from *Escherichia coli* serotype 0111:B4, *E. Coli* 055:B5, *Klebsiella pneumoniae, Pseudomonas aeruginosa, Salmonella minnesota,* and *Serratia marcescens* (Sigma Chemical Co., St. Louis, MO) were suspended in PBS at 5mg/ml and these stock solutions were stored at 4°C. The *E. Coli* 0111:B4 lipid A, and O-polysaccharide fractions were prepared by a method previously detailed by Dubois *et al* (25). For experiments, the LPS stock solutions were mixed with supplemented tissue culture media as described below. In those experiments where LPS preparations from diverse bacterial strains were simultaneously studied, equivalent amounts of LPS on a dry weight/weight basis could not be compared. This is because for each specific LPS, the length of the O-specific polysaccharide and lipid A acyl chains can markedly differ. However, all LPS regardless of the bacterial origin, contains at least one 2-keto-3-deoxyoctonic acid (KDO). Therefore, equivalent amounts of LPS can be determined by utilizing a method which targets this conserved structure, namely, the Karkhanis method of determining the percent KDO by optical density (26). The concentrations of each LPS was based on KDO content standardized to the KDO content of 10ng/ml of LPS derived from *E. coli* 0111:B4.

Endotoxin Neutralizing Protein (ENP): ENP was a gift from the Associates of Cape Cod (Woods Hole, MA). ENP was reconstituted at 1mg/ml in PBS, aliquoted, and stored at ~20°C. Polymyxin B (PMB) sulfate was purchased from Sigma and reconstituted at 25.8mg/ml for storage at 4°C.

EC Culture: Bovine pulmonary artery EC, obtained from the American Type Culture Collection (Rockville, MD), were cultured at 37 °C under 5% CO_2 in Dulbecco's Modified Eagle's Medium (Sigma) enriched with 20% fetal bovine serum (FBS) (Hyclone Laboratories, Inc., Logan, UT), 5 mM L-glutamine, nonessential amino acids, and vitamins, in the presence of penicillin (50 u/ml) and streptomycin (50 μg/ml) (Sigma). The cells were washed and gently detached with a brief (1-2 min) trypsin (0.5 mg/ml) (Sigma) exposure with gentle agitation followed immediately by trypsin-neutralization with FBS-containing medium. The cells were counted and suspended in medium for immediate seeding of tissue culture dishes or barrier function assay chambers.

Immunoblotting for Phosphotyrosines: EC were seeded in 100 mm cell culture dishes (Corning Inc., Corning, NY) at a density of 1.5 x 10^6 cells/dish and cultured for 72h. Monolayers were exposed to a range of LPS concentrations for varying exposure times. In certain experiments, LPS (100ng/ml, 1h) was introduced in combination with sodium orthovanadate (50, 100, 200, or 250μM) to maximize the LPS-induced elevated expression of phosphotyrosine-containing proteins. In some experiments, herbimycin A (1μM) or genistein (50μg/ml) were introduced 16h and 1h, respectively, prior to and throughout the 1 h study period. Following treatment, the cells were washed x2 with ice-cold PBS containing 1 mM vanadate. The cells were then lysed for 15 min with ice-cold modified RIPA lysis buffer [50 mM Tris-HCl (pH 8.0), 1% NP-40, 0.25% sodium deoxycholate, 150 mM NaCl, 1 mM ethylene glycol tetraacetic acid (EGTA), 1 mM phenylmethylsulfonyl fluoride (PMSF), 1 μg/ml leupeptin, 1 μg/ml

pepstatin, 1 μg/ml aprotinin, 1 μg/ml DNAse, 1 mM sodium orthovanadate, 1 mM NaF, 1 mM pyrophosphate, 1 mM phenylarsine oxide (PAO), 500 μM P-nitrophenyl phosphate, 1 mM dithiothreitol (DTT)]. The cells were scraped and transferred to a tube and centrifuged (16,000 g, 10 min, 4 °C). The supernatant was lyophilized and reconstituted in 500 μl of distilled water. EC lysates were resolved by SDS-PAGE on an 8-16% Tris-Glycine gradient gel (Novex Inc., San Diego, CA) using 25μg protein/lane, and transferred (30v x 3h) to polyvinylidene fluoride membrane (PVDF). The blot was blocked (3% dry milk in PBS,1h, RT) and incubated with biotinylated 4G10 anti-phosphotyrosine antibodies (0.7 μg/ml) (Upstate Biotechnology Inc., Lake Placid, NY), washed, and incubated with horseradish peroxidase (HRP)-conjugated streptavidin (0.5 μg/ml) (Upstate Biotechnology Inc.). The blot was then rinsed and developed with enhanced chemiluminescence (Amersham Life Sciences, Arlington Heights, IL) and exposed to Du Pont Reflection (NEF-406) film.

Assay of Transendothelial Albumin Flux: Transendothelial ^{14}C-bovine serum albumin (BSA) flux was assayed as previously described (10,23,24). Polycarbonate filters (13 mm diameter, 0.4 μm pore size) (Nuclepore Inc., Pleasanton, CA) were treated with 0.5% acetic acid (50 °C, 20 min), washed in distilled H_2O and immersed in boiling pigskin gelatin (Fisher Scientific, Pittsburgh, PA) 5 mg/L distilled H_2O for 60 min. The filters were then dried, glued to polystyrene chemotactic chambers (ADAPS, Inc., Dedham, MA), and gas sterilized with ethylene oxide. These chambers which served as the upper compartment for the assay chambers were inserted into wells of 24-well plates, each well containing 1.5 ml media and serving as the lower compartment of

the assay chamber. Each upper compartment was seeded with 2 x 10^5 EC in 0.5 ml media and cultured for 72h (37°C, 5% CO_2). We used ^{14}C-BSA (Sigma) with a specific activity of 30.1 μCi per mg protein as the tracer molecule. The baseline barrier function of each monolayer was determined by applying an equivalent and reproducible amount of ^{14}C-BSA (1.1 pmol/0.5 ml) to each upper compartment for 1h at 37°C, after which 0.5 ml from the lower compartment was added to 4.5 ml of Optifluor scintillation fluid (Packard Instruments Co., Downers Grove, IL) and counted in a liquid scintillation analyzer (Packard). Only endothelial monolayers retaining $\geq$97% of the ^{14}C-BSA were studied. The monolayers were then treated for 6h with LPS (10 or 100 ng/ml), genistein (50 μg/ml), herbimycin A (1 μM), PAO (0.1 μM), sodium orthovanadate (2.5 μM), or combinations of LPS and any one of the other agents. All inhibitors were introduced simultaneously with LPS except for herbimycin A and genistein, in which cases the cells were pretreated for 16 h and 0.5 h respectively, prior to the introduction of LPS. The concentrations of each inhibitor was chosen on the basis of its activity in the barrier function assay; the maximal subthreshold concentration of each inhibitor was chosen. Simultaneous controls with medium alone were also performed. Transfer of ^{14}C-BSA across EC monolayers was again assayed.

In other experiments, LPS structure-function studies using lipid A and polysaccharide fractions were performed. EC monolayers were exposed for 6h to increasing concentrations of either the lipid A or polysaccharide fraction. In other experiments, native LPS was coadministered with PMB. The ability of ENP to directly

neutralize LPS-induced barrier dysfunction was also studied. Here, monolayers were exposed for 6h to a fixed concentration of LPS (10ng/ml) in the presence of increasing concentrations of ENP (10ng/ml to 10μg/ml). The ability of ENP to protect against a range of endotoxins derived from diverse gram-negative bacterial strains was also studied.

F-Actin Epifluorescence Microscopy: To maintain EC monolayers under identical experimental conditions to our permeability assay, we used a previously described method to directly stain and visualize the monolayers on polycarbonate membrane filters (10). EC cultured to confluence on filters were exposed for 6 h to media alone, LPS (100 ng/ml), herbimycin A (1 μM), or LPS and herbimycin A. Herbimycin A was introduced 16h prior to the study period. The monolayers were fixed (3.7 % formaldehyde, 20 min), permeabilized (0.5% Triton X-100 in HEPES buffer, 5 min), and stained with fluorescein-phalloidin (1.65×10^{-7} M, 20 min)(Molecular Probes). The filters and their attached monolayers were mounted cell-side up on microscope slides and photographed through a Zeiss Axioscop 20 microscope (100 x oil, Plan Neofluar objective) equipped for epifluorescence.

G-Actin Quantification: Endothelial G-actin was measured using the DNAse 1 inhibition assay as previously described (10). The assay is based upon the ability of monomeric G-actin to inhibit DNAse hydrolysis of type 1 DNA into its component nucleotides. DNAse 1 obtained from bovine pancreas (Sigma, St. Louis, MO) was dissolved at 10 mg/ml in 0.125 M Tris-HCl (pH 7.5), 5 mM $MgCl_2$, 2 mM $CaCl_2$, 1 mM sodium azide, and 0.1 mM PMSF for enhanced stability. The stock solution was then

diluted 100x with 20 mM imidazole (pH 7.5), 30 mM NaCl, and 15% glycerol. Calf thymus type 1 DNA (Sigma) was used as a substrate for the DNAse 1. The fibrous DNA preparation was finely cut and suspended in 0.1 M Tris-HCl (pH 7.5), 4 mM $MgSO_4$, 1.8 mM $CaCl_2$, at a concentration of 80 μg/ml. The DNA was solubilized by gentle stirring at 4 °C for 48 h after which the solution was sequentially filtered through 0.45 and 0.22 μm pore size filters and stored at 4 °C. The DNAse 1 was mixed with DNA substrate in the cuvette of a Gilford response II spectrophotometer and the slope of the linear portion of the ΔA 260 recorded. Purified bovine skeletal muscle actin (Sigma) dissolved in 20 mM Tris-HCl (pH 7.5), 1 M sodium acetate, 1 mM $CaCl_2$, 1 mM adenosine triphosphate (ATP), and 0.75 M guanidine HCl, was used to create a standard curve for the standardization of the G-actin assay. EC monolayers grown in 6-well plates were exposed to media, herbimycin A, genistein, vanadate, PAO, or any combination of LPS and the preceding agents in a parallel manner to the conditions used to assay transendothelial flux. Following treatment, the monolayers were washed with Dulbecco's PBS and permeabilized with 0.5 ml of lysing buffer (Hank's Balanced Salt Solution with 1% Triton X-100, 2 mM $MgCl_2$, 2 mM EGTA, 150 mM NaCl, 0.2 mM ATP, 0.5 mM DTT, 0.1 mM PMSF, pH 7.6) per well for 5 min. The G-actin containing supernatants were then tested in the DNAse 1 inhibition assay to generate inhibitory activities that fell between 30 - 70 % inhibition; the range between which DNAse 1 inhibitory activity is directly proportional to monomeric G-actin. The inhibitory activities were interpolated to G-actin concentrations from the standard curve and expressed in microgram per milligram of total EC protein. Total EC protein

was determined by plating out additional EC in 6-well plates and subjecting them to identical conditions as those of the G-Actin or F-actin assay. The cells were then washed x2 in PBS and lysed for 15 min in 0.5 ml of 3% SDS, 1 mM DTT, 0.1 mM PMSF, 1 mM EDTA, 50 mM Tris-HCL, pH 8.0. Lysates were assayed for protein concentration with the standard Bio-Rad DC Protein Assay (Bio-Rad Chemical Division, Richmond , CA). Total endothelial protein was used to standardize both G- and F-actin measurements.

F-Actin Quantification: Endothelial F-actin was fluorimetrically measured as previously described (10). EC (3.8×10^5 cells in 2 ml media) were seeded into the wells of 6-well plates and cultured for 72 h (37 °C, 5% CO_2). The monolayers were exposed to conditions identical to those of the transendothelial albumin flux and G-actin assays with the notable exception that all of the monolayers were treated with 50 μg/ml cycloheximide for 30 min prior to and throughout the various treatment exposures as previously described (10). The monolayers were washed x2 with 75 mM KCl, 1 mM EGTA, 3 mM $MgSO_4$, 0.2 mM DTT, 10 mM imidazole, 10 μg/ml aprotinin, 0.1 mM PMSF, pH 7.2, and fixed with 3.7% formaldehyde for 15 min. Monolayers were permeabilized for 5 min with 0.2% Triton X-100 in the KCl buffer, washed x2 with the KCl buffer, and incubated with NBD-phallacidin (1 unit/well, 30 min) (Molecular Probes, Eugene, OR), washed x4 with PBS, and methanol extracted (overnight, -20 °C). Staining and extractions were performed in the dark. The fluorescent-labeled extracts were measured in a Perkin-Ekmer LS30 luminescence spectrometer at room temperature at 465 nm excitation (10 nm slit) and 535 nm emission (10 nm slit) and

expressed in arbitrary fluorescence units per mg total EC protein.

Phosphotyrosine Immunolocalization: As with the F-actin epifluorescence microscopy, EC monolayers were seeded under identical conditions to those of the transendothelial flux assay. Cells were treated with media or LPS (100 ng/ml) for increasing time intervals. After treatment, monolayers were washed 3x with ice cold PBS containing 1 mM vanadate. Cells were fixed for 20 min in 4% formaldehyde in PBS at room temperature. Cells were then washed twice with PBS, exposed to ice cold methanol for 6 min at -20 °C, and then washed x2 with 1% BSA in PBS. The monolayers were stored overnight in the 1% BSA-PBS solution at 4 °C. EC were subsequently exposed to 5 μg/ml of FITC-conjugated anti-phosphotyrosine (Upstate Biotechnology Inc.) for 1 h at room temperature in the dark. Monolayers were washed twice with 1% PBS-BSA followed by x3 washes with PBS. The filters were removed from the chambers, mounted cell-side up on microscope slides and visualized through a Zeiss Axioscop 20 microscope (100x oil, Plan Neofluar objective).

Immunoprecipitation of Phosphotyrosine-Containing Proteins and Paxillin: LPS-exposed EC were lysed with modified RIPA buffer and the lysates incubated overnight with either PY20 anti-phosphotyrosine antibody (5 μg/ml) (Transduction Laboratories, Lexington, KY) or anti-paxillin antibody (0.25 μg/ml) (Transduction Laboratories) at 4 °C. The resultant immune complexes were immobilized by incubation with anti-mouse IgG cross-linked to agarose (Sigma) for 2 h at 4 °C. The pellet was isolated following centrifugation, washed x3 with modified RIPA buffer, and boiled in sample buffer for 5 min. Proteins were resolved with SDS-PAGE and transferred onto PVDF as

described above. Select lanes of the blot were subsequently probed with a murine monoclonal antibody raised against paxillin (0.025 μg/ml) (Transduction Laboratories) followed by incubation with HRP-conjugated anti-mouse IgG (0.13 μg/ml) (Transduction Laboratories). Other lanes of the blot were probed with the biotinylated anti-phosphotyrosine antibody as described above. All lanes were then developed with enhanced chemiluminescence (Amersham Life Sciences).

Immunodepletion of Paxillin from Lysates Isolated from LPS-Exposed EC: LPS-exposed (100ng/ml, 1h) EC were lysed with modified RIPA buffer and the lysates incubated overnight with anti-paxillin antibody (1.25μg/ml) (Transduction Laboratories) at 4°C. The resultant immune complexes were immobilized by incubation with anti-mouse IgG cross-linked to agarose for 2h at 4°C. The paxillin-depleted supernatant (25μg/lane) and the paxillin-containing immunoprecipitate, along with whole cell lysates (25μg/lane) isolated from media and LPS-exposed EC were each resolved by SDS-PAGE and probed with anti-phosphotyrosine (4G10) antibodies as described above.

Phosphotyrosine Co-localization with Paxillin: EC monolayers were seeded under identical conditions to those of the transendothelial flux assay and treated for 1h with media alone or LPS (100 ng/ml). Monolayers were washed, fixed, and permeabilized under conditions identical to those for immunolocalization as described above, with the exception that 0.5% Triton X-100 in PBS was used to permeabilize the cells instead of ice cold methanol. Permeabilized EC were exposed to mouse anti-paxillin antibody (5 μg/ml) for 1 h, washed x3 with 1% BSA in PBS, and then incubated with Texas Red-conjugated sheep anti-mouse IgG (3 μg/ml) (Cappel/Organon Teknika Corp.,

Durham, NC). After vigorous washing, the monolayers were then exposed to FITC-conjugated anti-phosphotyrosine and subsequently visualized as described above.

Statistical Methods: Analysis of variance (ANOVA) was used to compare the mean responses among experimental and control groups for all experiments. The Scheffe F-test was used to determine between which groups significant differences existed. A p-value of <0.05 was considered significant.

RESULTS

Dose- and time-dependent effect of LPS on tyrosine phosphorylation of a 65 kDa protein: EC monolayers were exposed to varying concentrations of LPS for 1h. Lysates were resolved by SDS-PAGE, transferred, and probed with anti-phosphotyrosine antibodies. EC lysates from LPS-exposed cells revealed an increase in tyrosine phosphorylation of a protein of apparent molecular weight of 65 kDa (Fig. 1). The increased state of protein tyrosine phosphorylation was seen at LPS concentrations of $\geq$ 10 ng/ml after which the level of tyrosine phosphorylation appeared to plateau (Fig. 1A). EC monolayers were then exposed to a fixed LPS concentration (100 ng/ml) for increasing exposure times (Fig. 1B). LPS-induced elevation of phosphotyrosine-containing proteins was maximal at 30 and 60 min. At 2 h the difference in levels of tyrosine phosphorylation between EC exposed to LPS or media alone was diminished and by 4h, this difference was undetectable. In order to maximize LPS-induced protein tyrosine phosphorylation, EC were exposed to LPS (100 ng/ml, 1h) in the presence and absence of the protein tyrosine phosphatase (PTP) inhibitor, sodium orthovanadate (Fig. 1C). In the face of PTP inhibition, protein tyrosine phosphorylation in LPS-exposed EC was increased compared to EC exposed to LPS alone, but not increased relative to simultaneous media controls in the presence of PTP inhibition.

Effect of PTK inhibitors on LPS-induced increases in transendothelial ^{14}C-BSA flux: The mean ($\pm$ SE) pretreatment baseline ^{14}C-BSA flux across monolayers was 0.012 pmol/h $\pm$ 0.0005 (n = 93) (Fig. 2A). LPS exposure (100 ng/ml, 6 h) resulted in an

~ two-fold increase in transendothelial flux as compared to media controls. The introduction of herbimycin A (1 μM) or genistein (50 μg/ml) in combination with LPS resulted in 100% and 77% protection against the LPS-induced increments in albumin flux, respectively. Transendothelial flux across EC monolayers exposed to either one of these functionally and structurally dissimilar PTK inhibitors alone did not significantly differ from the flux across media control monolayers.

Effect of PTK inhibitors on LPS-induced protein tyrosine phosphorylation: The ability of herbimycin A and genistein to each specifically inhibit tyrosine phosphorylation of the 65 kDa protein in response to LPS was studied. To enhance the phosphotyrosine signal, monolayers were exposed to the PTP inhibitor, sodium orthovanadate (see Fig. 1C). Western blot analysis probing LPS-exposed EC for phosphotyrosines in the presence and absence of PTK inhibitors was performed (Fig. 2B). Either herbimycin A or genistein clearly prevented the LPS-induced elevation of tyrosine phosphorylation of the 65 kDa protein.

Effect of PTK inhibition on LPS-induced intercellular gap formation: F-actin probed EC monolayers exposed for 6h to media alone (Fig. 3A), herbimycin A (1 μM) (Fig. 3B), LPS (100 ng/ml) (Fig. 3C), or LPS in combination with herbimycin A (Fig. 3D) were photographed through an epifluorescence microscope. The medium control monolayers exhibited tight cell-to-cell apposition without intercellular gaps (Fig. 3A) as did the monolayers exposed to herbimycin A (Fig. 3B). LPS-treated monolayers displayed intercellular gap formation (Fig. 3C). The introduction of herbimycin A

blocked the formation of these intercellular gaps in response to LPS (Fig. 3D).

Effect of PTK inhibition on LPS-induced increments in the EC G-actin pool: The effects of LPS and PTK inhibition on the EC G-actin pool was studied (Fig. 4A). G-actin was expressed as micrograms of G-actin per milligram total EC protein. EC monolayers were exposed for 6 h to media alone, herbimycin A (1μM), genistein (50 μg/ml), LPS (100 ng/ml), or LPS in combination with either herbimycin A or genistein. The G-actin pools in EC exposed to either herbimycin A or genistein were not significantly different from their respective media controls. LPS increased the G-actin pool compared to simultaneous media controls and this increase could be blocked by either herbimycin A or genistein. In fact, when LPS was coadministered with genistein, the G-actin pool was not greater than the simultaneous media control.

Effect of PTK inhibition on LPS-induced decrements in the EC F-actin pool: It has been previously reported that the LPS-induced increments in the G-actin pool is due, in part, to the depolymerization of F-actin (10). We therefore examined the role of PTK inhibition in modulating LPS-induced decrements of the F-actin pool. All EC monolayers were treated with cycloheximide (50 μg/ml) for 30 min prior to and throughout the study period to block *de novo* actin synthesis as previously described (10). F-actin was expressed as arbitrary fluorescence units per milligram of total EC protein. F-actin in EC exposed to either herbimycin A or genistein were not significantly different from their respective media controls (Fig. 4B). Monolayers treated with LPS (100 ng/ml, 6 h) had significantly decreased F-actin compared to their

simultaneous media controls (Fig. 4B). PTK inhibition with either herbimycin A or genistein significantly protected against the LPS-induced F-actin decrement. In fact, EC coadministered LPS in the presence of herbimycin A were not significantly different than either the simultaneous media or herbimycin A controls.

Effect of PTP inhibition on LPS-induced increases in transendothelial ^{14}C-BSA flux: Since PTK inhibition blocked monolayer disruption by LPS, we studied whether PTP inhibition enhanced the LPS effect. Exposure to vanadate or PAO alone did not significantly alter albumin flux as compared to their respective media controls. Coadministration of either vanadate (2.5 μM) or PAO (0.1 μM) with LPS (10 ng/ml, 6h) significantly enhanced the LPS-induced increment in transendothelial flux of ^{14}C-BSA compared to monolayers exposed to LPS alone (Fig. 5).

Effect of PTP inhibition on LPS-induced increases of the EC G-actin pool: After finding that PTP inhibition could enhance the LPS-induced permeability of EC monolayers, we examined whether vanadate (2.5 μM) or PAO (0.1 μM) could enhance the G-actin increase that results from LPS treatment. The introduction of either inhibitor in combination with LPS (10 ng/ml, 6 h) resulted in a significantly greater increase in the G-actin pool compared to LPS treatment alone (Fig. 6). Monolayers exposed to vanadate or PAO alone did not demonstrate differences in G-actin compared to the simultaneous media controls.

Immunolocalization of phosphotyrosine-containing proteins: EC monolayers were

exposed for 1h to media or LPS (100 ng/ml), probed for phosphotyrosine-containing proteins, and visualized through an epifluorescence microscope (Fig. 7). Phosphotyrosine-containing proteins were immunolocalized to the intercellular boundaries as well as to plaque-like structures.

Immunoprecipitation of phosphotyrosine-containing proteins and paxillin: Phosphotyrosine-containing proteins and paxillin were immunoprecipitated from EC monolayers exposed to LPS (100 ng/ml, 1 h), resolved by SDS-PAGE, transferred to PVDF, and subsequently probed for paxillin or tyrosine phosphorylated residues (Fig. 8). Both the 65 kDa tyrosine phosphorylated protein and paxillin isolated from the LPS-exposed EC, comigrated to the same position on the blot.

Identification of Paxillin as the 65kDa Phosphotyrosine-Containing Protein: Phosphotyrosine-containing proteins and paxillin were immunoprecipitated from EC monolayers exposed to LPS (100ng/ml, 1h), resolved by SDS-PAGE, transferred to PVDF, and subsequently probed for paxillin or tyrosine phosphorylated proteins (Fig. 8A). Both the 65kDa tyrosine-phosphorylated protein and paxillin isolated from the LPS-exposed EC, comigrated to the same position on the blot. In other experiments, the supernatants from lysates immunodepleted of paxillin (ID) were resolved by SDS-PAGE (Fig. 8B). Probing with anti-phosphotyrosine antibody demonstrated that the 65kDa tyrosine-phosphorylated band disappears after paxillin is immunodepleted. The band is recovered by resolving the isolated paxillin that was immunoprecipitated (IP) (Fig. 8B).

Co-localization of phosphotyrosine-containing proteins and paxillin: EC monolayers were exposed to media or LPS (100 ng/ml, 1 h), and probed for paxillin (shown as red) and phosphotyrosine-containing proteins (shown as green) (Fig. 9). As visualized through an epifluorescence microscope, the probes for paxillin and phosphorylated tyrosine residues co-localized (shown as yellow).

LPS Structure-function studies of LPS-induced endothelial barrier dysfunction: A 6h exposure to increasing concentrations of lipid A caused dose-dependent increases in ^{14}C-BSA flux across EC monolayers whereas the O-specific polysaccharide fraction did not (Figure 10A). The mean ($\pm$SE) pretreatment baselines for monolayers prior to exposure to either lipid A or O-specific polysaccharide fractions were 0.016$\pm$0.002 pmol/h and 0.013$\pm$0.002, respectively. The mean ($\pm$SE) ^{14}C-BSA flux across naked filters without endothelial monolayers was 0.215$\pm$0.015 pmol/h. The lowest lipid A concentration that caused a significant ($p<0.001$) increase in ^{14}C-BSA flux compared with the simultaneous medium control was 15ng/ml. Dose-dependent increments were seen at each lipid A concentration up to 15μg/ml, the maximum concentration tested. In contrast, the polysaccharide fraction at concentrations up to 15μg/ml failed to increase endothelial monolayer permeability compared to the simultaneous media control.

The ability of PMB to block native LPS-induced barrier dysfunction was also studied (Figure 10B). ^{14}C-BSA flux was assayed immediately after a 6h exposure to medium alone, LPS (10ng/ml), PMB (1000ng/ml), or LPS coadministered with PMB.

LPS increased ^{14}C-BSA flux compared to the simultaneous medium control, whereas PMB alone did not. PMB at a PMB:LPS ratio of 100:1 protected against the LPS effect, returning barrier function to the medium control levels.

Effect of ENP on LPS-induced changes in transendothelial ^{14}C-BSA flux: ENP protected against LPS-induced barrier dysfunction (Figure 11). Transendothelial albumin flux was assayed immediately after 6h exposures to medium alone, LPS (10ng/ml), or LPS coadministered with increasing concentrations of ENP (1-1000ng/ml). Again, LPS (10ng/ml) increased ^{14}C-BSA flux compared to the simultaneous medium control. Protection against LPS-induced increases in ^{14}C-BSA flux by coadministration of ENP was dose-dependent. ENP $\geq$10ng/ml significantly decreased LPS-induced barrier dysfunction. Maximum protection was seen with concentrations of ENP$\geq$100ng/ml (i.e., ENP:LPS ratio of 10:1), reducing ^{14}C-BSA flux to that seen for the medium controls.

Effect of ENP on LPS-induced tyrosine phosphorylation of EC proteins: Lysates obtained from EC exposed for 1h to medium alone, ENP (100ng/ml), LPS (10ng/ml), or LPS coadministered with ENP, were resolved by SDS-PAGE, transferred to PVDF, and probed for phosphotyrosine-containing proteins. LPS (10ng/ml) increased tyrosine phosphorylation of a 65kDa phosphotyrosine-containing protein (Figure 12). Coadministration of ENP with the LPS reduced the level of phosphotyrosine signal of the band compared to that seen for the media control.

EC monolayers exposed to medium alone, ENP (100ng/ml), LPS (10ng/ml), or LPS coadministered with ENP were probed with a FITC-conjugated anti-phosphotyrosine antibody, processed for epifluorescence microscopy, and photographed. At 1h, the

LPS positive control (Figure 13C) displayed an increase in phosphotyrosine-containing proteins immunolocalized to the cell periphery, compared to both medium and ENP controls (Figure 13A and 13B, respectively). Monolayers treated with both ENP and LPS (Figure 13D) could not be distinguished from either the medium or ENP controls.

Effects of ENP on the LPS-induced changes in the F- and G-actin pools: The effect of ENP on the LPS induced decrement in EC F-actin, expressed as fluorescence units/mg total EC protein, was studied (Figure 14A). There were no significant differences between the medium and ENP controls. A 6h exposure to LPS (10ng/ml) significantly ($p<0.0011$) decreased F-actin compared to either the simultaneous medium or ENP (1μg/ml) controls. ENP coadministered with LPS significantly ($p<0.0017$) reduced the LPS-induced F-actin decrement compared to LPS alone. In addition, LPS coadministered with ENP was not significantly decreased compared to the medium control.

The effect of ENP on the LPS-induced increment in G-actin, expressed in μg/mg total EC protein, was also studied (Figure 14B). A 6h exposure to LPS (10ng/ml) significantly (0.0001) increased G-actin compared to either the simultaneous medium or ENP (100ng/ml) controls. ENP coadministered with LPS significantly ($p<0.0001$) reduced the LPS-induced G-actin increase compared to LPS alone. In addition, this reduction was complete, reducing G-actin to the basal levels seen in the medium control. Therefore, LPS provokes reciprocal changes in the F- and G-actin pools indicative of EC actin depolymerization and ENP completely blocks this F- to G-actin shift.

Effect of ENP on LPS-induced intercellular gap formation: The F-actin organization of EC monolayers exposed to medium, ENP (100ng/ml), LPS (10ng/ml), or LPS coadministered with ENP was investigated (Figure 15). EC exposed to either medium or ENP contained continuous transcytoplasmic actin filaments and tight cell-to-cell apposition without intercellular gaps (Figures 15A and 15B). After a 6h exposure to LPS, intercellular gaps could be seen throughout the monolayer (Figure 15C). Monolayers exposed to LPS coadministered with ENP were similar in appearance to the medium and ENP controls; they contained continuous transcytoplasmic actin cables and tight cell-to-cell apposition (Figure 15D).

ENP protects against a range of LPS preparations derived from diverse gram-negative bacterial strains: ENP completely protected against loss of barrier function in response to a variety of LPS preparations normalized on the basis of KDO content to 10ng/ml of LPS derived from *E. Coli* O111:B4 (Figure 16). Monolayers were assayed for ^{14}C-BSA flux immediately after 6h exposures to medium, LPS derived from *E. Coli* O111:B4, *E. Coli* 055:B5, *Klebsiella pneumonia, Pseudomonas aeruginosa, Salmonella minnesota,* or *Serratia marcescens*, or an equivalent concentration of each LPS type coadministered with ENP (100ng/ml). All endotoxins, except that derived from *S. marcescens*, induced equivalent increments in ^{14}C-BSA. Again, ENP reduced barrier dysfunction induced by LPS derived from *E. Coli* O111:B4 to the medium control level. Further, ENP significantly reduced to media control levels increases in ^{14}C-BSA flux in response to all endotoxins tested.

CONCLUSIONS:

1. LPS induces tyrosine phosphorylation of an EC protein in a dose- and time-dependent manner. The phosphoprotein has a MW ≈ 65kDa and has now been identified as the focal adhesion component, paxillin. This effect appears after an LPS exposure time of 0.5-1.0h to LPS concentrations of $\geq$10ng/ml.
2. The phosphotyrosine-containing proteins in LPS-exposed EC monolayers could be immunolocalized to the intercellular boundaries as well as to plaque-like structures.
3. The phosphotyrosine-containing proteins restricted to the plaque-like structures co-localized with paxillin.
4. Tyrosine kinase inhibition protects against: (a) LPS-induced EC actin depolymerization i.e. an increase in the G-actin pool with a reciprocal decrease in the F-actin pool, (b) LPS-induced intercellular gap formation, and (c) LPS-induced loss of endothelial barrier function.
5. In contrast, tyrosine phosphatase inhibition enhances: (a) LPS-induced EC actin depolymerization, and (b) LPS-induced loss of endothelial barrier function
6. Endotoxin neutralizing protein (ENP) at an ENP:LPS ratio of 10:1 blocked LPS-induced tyrosine phosphorylation, actin depolymerization, intercellular gap formation, and loss of barrier function.
7. ENP cross-protects against loss of barrier function in response to LPS derived from diverse gram-negative bacteria.

SUMMARY: LPS induces tyrosine phosphorylation of an EC protein(s), paxillin, that leads to actin depolymerization and intercellular gap formation which provides a transendothelial paracellular pathway through which macromolecules can flux. An intervention that specifically targets the lipid A portion of the LPS molecule completely blocks these LPS-induced tyrosine phosphorylation-dependent signaling events, actin reorganization, and opening of the paracellular pathway..

REFERENCES:

1. Morrison, D.C., C.A. Dinarello, R.S. Munford, C. Natanson, R. Danner, M. Pollack, J.J. Spitzer, R.J. Ulevitch, S.N. Vogel, and E. McSweegan. 1994. Current status of bacterial endotoxins. *ASM News*. 60:479-484.

2. Danner, R.L., R.J. Elin, J.M. Hosseini, R.A. Wesley, J.M. Reilly, and J.E. Parillo. 1991. Endotoxemia in human septic shock. *Chest*. 99:169-175.

3. Schumann, R.R., N. Lamping, C. Kirshning, H.P. Knopf, A. Hoess, and F. Herrmann. 1994. Lipopolysaccharide binding protein: its role and therapeutical potential in inflammation and sepsis. *Biochem. Soc. Trans*. 22:80-82.

4. Brigham, K.L., and B. Meyrick. 1986. Endotoxin and lung injury. *Am. Rev. Respir. Dis.* 133:913-927.

5. Brandtzaeg, P., P. Kierulf, P. Gaustad, A. Skulberg, J.N. Bruun, S. Halvorsen, and E. Sorensen. 1989. Plasma endotoxin as a predictor of multiple organ failure and death in systemic meningococcal disease. *J. Infect. Dis.* 159:195-204.

6. Ziegler, E.J., J.A. McCutchan, J. Fierer, M.P. Glauser, J.C. Sadoff, H. Douglas, and A.I. Braude. 1982. Treatment of gram-negative bacteremia and shock with human antiserum to a mutant *Escherichia coli*. *N. Eng. J. Med.* 307:1225-1230.

7. Opal, S.M., C.J. Fisher, A.S. Cross, J.E. Palardy, D.L. Hoover, M.N. Marra, and R.W. Scott. 1992. Bactericidal/permeability-increasing protein as an anti-endotoxin therapeutic agent: comparisons with anti-core glycolipid polyclonal antibody therapy. *Clin. Res.* 40:213A.

8. Desch, C.E., P. O'hara, and J.M. Harlan. 1989. Anti-lipopolysaccharide factor from horseshoe crab, *Tachpleus tridentatus*, inhibits lipopolysaccharide activation of cultured human endothelial cells. *Infect. Immun.* 57:1612-1614.

9. Meyrick, B.O. 1986. Endotoxin-mediated pulmonary endothelial cell injury. *FASEB J.* 45:19-24.

10. Goldblum, S.E., X. Ding, T.W. Brann, and J. Campbell-Washington. 1993. Bacterial lipopolysaccharide induces actin reorganization, intercellular gap formation, and endothelial barrier dysfunction in pulmonary vascular endothelial cells: concurrent F-actin depolymerization and new actin synthesis. *J. Cell. Physiol.* 157:13-23.

11. Seifert, P.S., N. Haeffner-Cavaillon, M.D. Appay, and M.D. Kazatchkine. 1991. Bacterial lipopolysaccharides alter human endothelial cell morphology in vitro independent of cytokine secretion. *J. Lab. Clin. Med.* 118:563-569.

12. Garcia, J.G., and K.L. Schaphorst. 1995. Regulation of endothelial cell gap formation and paracellular permeability. *J. Invest. Med.* 43:117-126.

13. Dejana, E., M. Corada, and M.G. Lampugnani. 1995. Endothelial cell-to-cell junctions. *FASEB J.* 9:910-918.

14. Caveda, L., M. Corada, I.M. Padura, A.D. Maschio, F. Breviario, M.G. Lampugnani, and E. Dejana. 1994. Structural characteristics and functional role of endothelial cell to cell junctions. *Endothelium.* 2:1-10.

15. Volberg, T., Y Zick, R. Dror, I. Sabanay, C. Gilon, A. Levitzki, and B. Geiger. 1992. The effect of tyrosine-specific protein phosphorylation on the assembly of adherens-type junctions. *EMBO Journal.* 11:1733-1742.

16. Ulevitch, R.J., and P.S. Tobias. 1994. Recognition of endotoxin by cells leading to transmembrane signaling. *Curr. Opin. Immunol.* 6:125-130.

17. Arditi, M., J. Zhou, M. Torres, D.L. Durden, M. Stins, and K.S. Kim. 1995. Lipopolysaccharide stimulates the tyrosine phosphorylation of mitogen-activated protein kinases p44, p42, and p41 in vascular endothelial cells in a soluble CD14-dependent manner. *J. Immunol.* 155:3994-4003.

18. Melzig, M.F., and R. Loose. 1995. Investigations into the mechanism of toxicity of lipopolysaccharide (LPS) in bovine aortic endothelial cells. *Pharmazie.* 50:558-560.

19. Novogrodsky, A., A. Vanichkin, M. Patya, A. Gazit, N. Osherov, and A. Levitzki. 1994. Prevention of lipopolysaccharide-induced lethal toxicity by tyrosine kinase inhibitors. *Science.* 264:1319-1322.

20. Alpert G, G. Baldwin, C. Thompson, N. Wainwright, T.J. Novitsky, Z. Gillis, J. Parsonnet, G. Fleisher, and G. Siber. 1992. Limulus antilipopolysaccharide factor protects rabbits from menigococcal endotoxin shock. *J. Infect. Dis.* 165:494-500.

21. Fletcher M., T. Mckena, J. Quance, N. Wainwright, and T. Williams. 1993. Lipopolysaccharide detoxification by endotoxin neutralizing protein. *J. Sur. Res.* 55:147-154.

22. Hoess A., S. Watson, G. Siber, and R. Liddington. 1993. Crystal structure of endotoxin-neutralizing protein from the horseshoe crab, Limulus anti-LPS factor, at 1.5 A resolution. *EMBO J.* 12:3351-3356.

23. Kuppermann N., D. Nelson, R. Saladino, C. Thompson, F. Sattler, T. Novitsky, G. Fleisher, and G. Siber. 1994. Comparison of a recombinant endotoxin-neutralizing

protein with a human monoclonal antibody to endotoxin for the treatment of *Escherichia coli* sepsis in rats. *J. Infect. Dis.* 170:630-635.

24. Warren W., M. Glennon, N. Wainwright, S. Amato, K. Black, S. Kirsch, G. Riveau, R. Whyte, W. Zapol, and T. Novitsky. 1992. Binding and neutralization of endotoxin by *limulus* antipopolysaccharide factor. *Infect. Immun.* 60:2506-2513.

25. Dubois M., K. Giles, J. Hamilton, P. Rebers, and F. Smith. 1956. Colorometric method for determination of sugars and related substances. *Anal. Chem.* 28:350-356.

26. Karhanis Y., J. Zeltner, J. Jackson, and D. Carlo. 1978. A new method for the determination of KDO in LPS. *Anal. Biochem.* 85:595-601.

APPENDIX

Figures and Figure Legends 1-16

Figure 1: LPS-Induced Tyrosine Phosphorylation of EC Proteins. Whole cell lysates were isolated from EC incubated with: increasing concentrations of LPS for 1 h (A), LPS (100 ng/ml) (+) or media alone (-) for increasing exposure times (B), or increasing concentrations of the PTP inhibitor, sodium orthovanadate, in both the presence (+) and absence (-) of LPS (100 ng/ml) (C). The lysates were resolved by SDS-PAGE, transferred to PVDF, and probed for phosphotyrosines. Approximate molecular weights (kilodaltons) are indicated by arrows on the left. Each blot shown is representative of three separate experiments.

Figure 2: The Effects of PTK Inhibition on LPS-Induced Barrier Disruption and Protein Tyrosine Phosphorylation. Mean (± SE) transendothelial ^{14}C-BSA flux across monolayers (A) and protein tyrosine phosphorylation (B) were assayed following exposure for 6 h and 1 h, respectively, to varying combinations of: media, LPS (100 ng/ml), herbimycin A (Herb A) (1 μM), and genistein (Gen) (50 μg/ml). For both studies, herbimycin A and genistein were introduced at 16 h and 0.5 h, respectively, prior to the study period. Transendothelial flux is expressed in pmol/h and the mean (± SE) baseline barrier function is indicated by the closed bar. * = significantly increased compared to simultaneous media controls. ** = significantly decreased compared to monolayers exposed to LPS alone. For Western blot analysis of protein tyrosine phosphorylation, EC monolayers were exposed to the varying conditions in the presence of sodium orthovanadate (250 μM) to optimize the phosphotyrosine signal (B). The EC whole cell lysates were then resolved by SDS-PAGE, transferred to PVDF, and probed for phosphotyrosines. This is a representative blot of three separate experiments.

Figure 3: The Effect of PTK Inhibition on LPS-Induced Intercellular Gap Formation. EC monolayers grown on filters were exposed for 6 h to media (A), herbimycin A (1 μM) (B), LPS (100 ng/ml) (C), or LPS in combination with herbimycin A (D). Herbimycin A was introduced 16 h prior to the 6 h study period. The monolayers were fixed, permeabilized, stained with fluorescein-phalloidin, and examined by epifluorescence microscopy. Arrows point to intercellular gaps. x 800.

Figure 4: The Effect of PTK Inhibition on both the LPS-Induced Increments of the G-Actin Pool and Decrements of the F-Actin Pool. For G- and F-actin measurements, monolayers were exposed for 6 h to media, LPS (100 ng/ml), herbimycin A (Herb A) (1 μM), genistein (Gen) (50 μg/ml), or combinations of LPS with herbimycin A or genistein. Cells that were exposed to herbimycin A or genistein were pretreated for 16 h and 0.5 h, respectively. For the quantitation of the G-actin pool, EC were permeabilized and the G-actin-containing supernatants tested in the DNAse I inhibition assay standardized to pure G-actin (A). Each bar represents the mean ($\pm$SE) G-actin in micrograms per milligram of total EC protein. *n* for each group is indicated within each bar. * = significantly increased compared to the simultaneous media control. ** = significantly decreased compared to LPS alone. For the F-actin studies, monolayers were fixed, permeabilized, incubated with NBD-phallacidin, and extracted in methanol (B). The extracts were spectrofluorimetrically assayed and F-actin concentrations were expressed as mean ($\pm$SE) fluorescent units per milligram of total EC protein. * = significantly decreased as compared to the simultaneous media control. ** = significantly increased compared to LPS alone.

Figure 5: The Effects of PTP Inhibition on LPs-induced Increments of Transendothelial ^{14}C-BSA Flux. Mean (±SE) transendothelial ^{14}C-BSA flux across monolayers exposed for 6 h to media, LPS (10 ng/ml), vanadate (Van) (2.5 μM), PAO (0.1 μM), or combinations of LPS with vanadate or PAO is expressed in pmol/h. The mean (± SE) baseline barrier function is indicated by the closed bar. * = significantly increased compared to simultaneous media control. ** = significantly increased compared to LPS alone.

Figure 6: The Effects of PTP Inhibition on LPS-Induced Increments in the G-Actin Pool. For G-actin measurements, EC were exposed to media, LPS (10 ng/ml), vanadate (Van) (2.5 μM), PAO (0.1 μM), or combinations of LPS with vanadate or PAO. EC were then permeabilized and the G-actin-containing supernatants tested in the DNAse 1 inhibition assay standardized to pure G-actin. Each bar represents the mean (±SE) G-actin in micrograms per milligram of total EC protein. * = significantly increased compared to simultaneous media control. ** = significantly increased compared to LPS alone.

Figure 7: Immunolocalization of Phosphotyrosine-Containing Proteins. EC monolayers grown on filters were exposed to media or LPS (100 ng/ml) for increasing time intervals. Monolayers were subsequently fixed, permeabilized, stained with FITC-conjugated anti-phosphotyrosine antibody, and visualized through an epifluorescence microscope. x 840.

Figure 8: Immunoprecipitation of Phosphotyrosine-Containing Proteins and Paxillin in EC Exposed to LPS. (A) EC were exposed to LPS (100 ng/ml, 1 h) and lysed with a modified RIPA buffer. The EC lysates were incubated with either anti-phosphotyrosine

(PY20) or anti-paxillin (PAX) antibodies. The immunoprecipitates were resolved by SDS-PAGE and transferred onto PVDF. The blots were probed with antibodies against phosphotyrosine (4G10) or paxillin, followed by incubation with HRP-conjugated anti-murine antibody, and developed with enhanced chemiluminescence. (B) Lysates from EC exposed to LPS (100ng/ml) or media alone were processed for immunoblotting for phosphotyrosine-containing proteins. A portion of the lysate from LPS-exposed EC was immunoprecipitated with anti-paxillin antibody, and both the immunoprecipitate (IP) and the immunodepleted supernatant (ID) were resolved on SDS-PAGE, transferred to PVDF, and probed with antiphosphotyrosine antibody. IP = immunoprecipitation. IB = immunoblotting. ID = immunodepletion.

Figure 9. Co-localization of Paxillin and Phosphotyrosine-containing Proteins. EC monolayers grown on filters were exposed for 1 h to either media or LPS (100 ng/ml). The monolayers were then fixed, permeabilized, incubated with murine anti-paxillin antibody, washed, and subsequently incubated with Texas Red-conjugated anti-mouse IgG. After vigorous washing, the monolayers were then stained with FITC-conjugated anti-phosphotyrosine antibody, and visualized through an epifluorescence microscope. Green indicates phosphotyrosine-containing proteins, red indicates paxillin, and yellow indicates co-localization of the two probes. x 850.

Figure 10. The effects of LPS Fractions on Transendothelial ^{14}C-BSA Flux. (A) Transendothelial ^{14}C-BSA flux was determined across monolayers exposed for 6h to increasing concentrations of either the lipid A fraction (gray bars) or the O-specific polysaccharide fraction (open bars). All bars represent mean ($\pm$SE) transendothelial

^{14}C-BSA flux in pmol/h. Mean (±SE) pretreatment baseline ^{14}C-BSA flux across monolayers exposed to both lipid A and O-specific polysaccharide fractions (closed and horizontal-striped bars, respectively) as well as mean (±SE) ^{14}C-BSA flux across naked filters (cross-hatched bar) are presented. (B) EC monolayers were assayed for transendothelial ^{14}C-BSA flux immediately after 6h exposures to medium alone (open bar), PMB (1000ng/ml) (horizontal striped bar), LPS (10ng/ml) (cross-hatched bar), or LPS coadministered with PMB (gray bar). Mean (±SE) pretreatment baseline ^{14}C-BSA flux is represented by the closed bar. n, number of monolayers studied. * Significantly increased compared to simultaneous media control. ** significantly decreased compared to LPS alone but not significantly elevated compared to the media control.

Figure 11. The Dose-dependent effect of ENP on LPs-Induced Barrier Dysfunction. Mean (±SE) pretreatment baseline (closed bar) was determined prior to EC monolayer treatment. Transendothelial ^{14}C-BSA flux was determined across monolayers exposed for 6h to media (open bar), ENP (10^4ng/ml) (gray bar), LPS (10ng/ml) (cross-hatched bar), or LPS coadministered with increasing concentrations of ENP (vertical striped bars). *Significantly increased compared to medium control. ** Significantly decreased compared to LPS alone but significantly elevated compared to the media control. ***Significantly decreased compared to LPS alone but not significantly elevated compared to the media control.

Figure 12. The Effect of ENP on LPs-Induced Tyrosine Phosphorylation of a 65kDa EC protein. EC monolayers were exposed for 1h to media, ENP (1μg/ml), LPS (10ng/ml), or LPS coadministered with ENP. The EC lysates were resolved by SDS-PAGE, transferred to PVDF, and the blots probed for phosphotyrosines.

Figure 13. The Effect of ENP on Phosphotyrosine-Containing Proteins in LPS-Exposed EC. EC monolayers grown on filters were exposed for 1h to media (A), ENP (100ng/ml) (B), LPS (10ng/ml) (C), or LPS coadministered with ENP (D). The monolayers were fixed, probed with FITC-conjugated anti-phosphotyrosine antibody, and photographed through an epifluorescence microscope . (x 800).

Figure 14. The effect of ENP on LPs-Induced Changes in the F- and G-actin Pools. For G- and F-actin measurements, monolayers were exposed for 6h to media alone (open bar), ENP (1000ng/ml) (gray bar), LPS (10ng/ml) (cross-hatched bar), or LPS coadministered with ENP (vertical striped bar). (A), For the F-actin studies, monolayers were fixed, permeabilized, incubated with NBD-phallacidin, and extracted with methanol. The extracts were spectrofluorimetrically assayed and F-actin concentrations expressed as mean ($\pm$SE) fluorescent units per mg of total EC protein. *Significantly decreased compared to media control. **Significantly increased compared to F-actin from EC treated with LPS alone. (B), for the quantitation of the G-actin pool, EC were permeabilized and the G-actin containing supernatants tested in the DNAse I inhibition assay standardized to pure G-actin. Each bar represents the mean ($\pm$SE) EC G-actin expressed in μg/mg total EC protein. The *n* for each group is indicated within each bar. * significantly increased compared to media control. **Significantly decreased compared to G-actin from EC treated with LPS alone.

Figure 15. Effect of ENP on LPS-Induced Intercellular Gap Formation. EC monolayers grown on filters were exposed for 6h to medium (A), ENP (100ng/ml) (B), LPS (10ng/ml) (C), or LPS coadministered with ENP (D). The monolayers were fixed (1%

formaldehyde in PBS), permeabilized (3% Triton X100), stained with fluorescein-phalloidin, and examined by epifluorescence microscopy. (x 800).

Figure 16. ENP Cross-Protects Against a Wide Variety of Endotoxins. Vertical bars represent the mean (±SE) transendothelial ^{14}C-BSA flux in pmol/h immediately after 6h exposures to media, (open bars), equivalent concentrations on the basis of KDO content of LPS derived from *E. coli* O111:B4 (10ng/ml), *E. coli* 055:B5, *K. pneumoniae, P. aeruginosa, S. minnesota,* or *S. marcescens* (crosshatched bars), or these same LPS preparations coadministered with ENP (100ng/ml) (gray bars). *Significantly decreased compared to LPS alone at $p<0.05$ but not significantly increased compared to medium control.

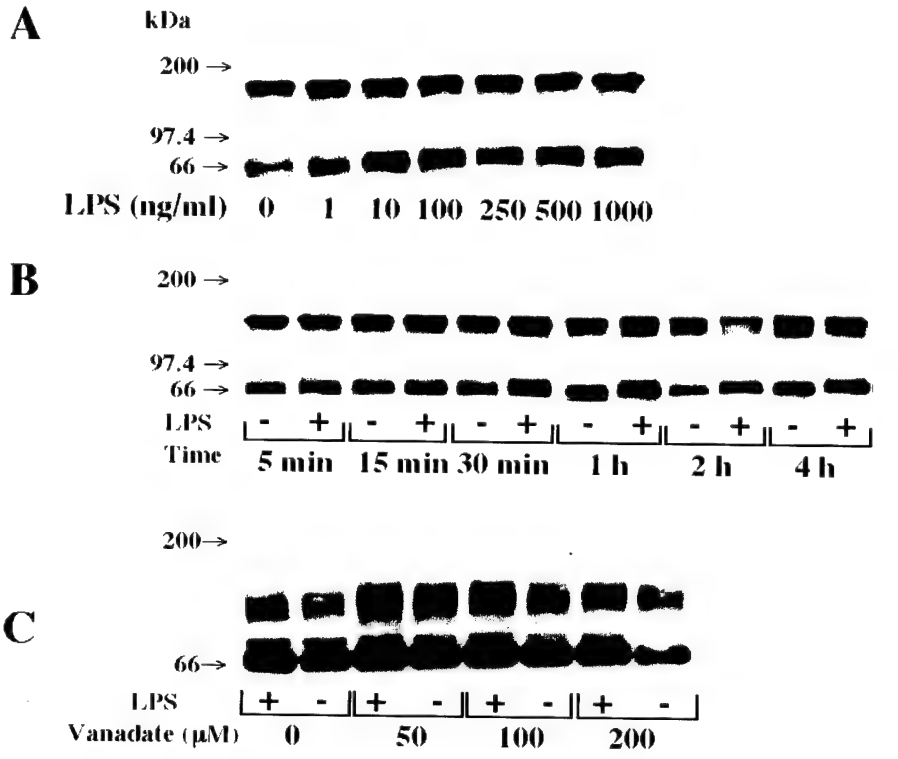
A
kDa
200 →
97.4 →
66 →
LPS (ng/ml) 0 1 10 100 250 500 1000
B
200 →
97.4 →
66 →
LPS - + - + - + - + - + - +
Time 5 min 15 min 30 min 1 h 2 h 4 h
C
200→
66→
LPS + - + - + - + -
Vanadate (μM) 0 50 100 200

Figure 1

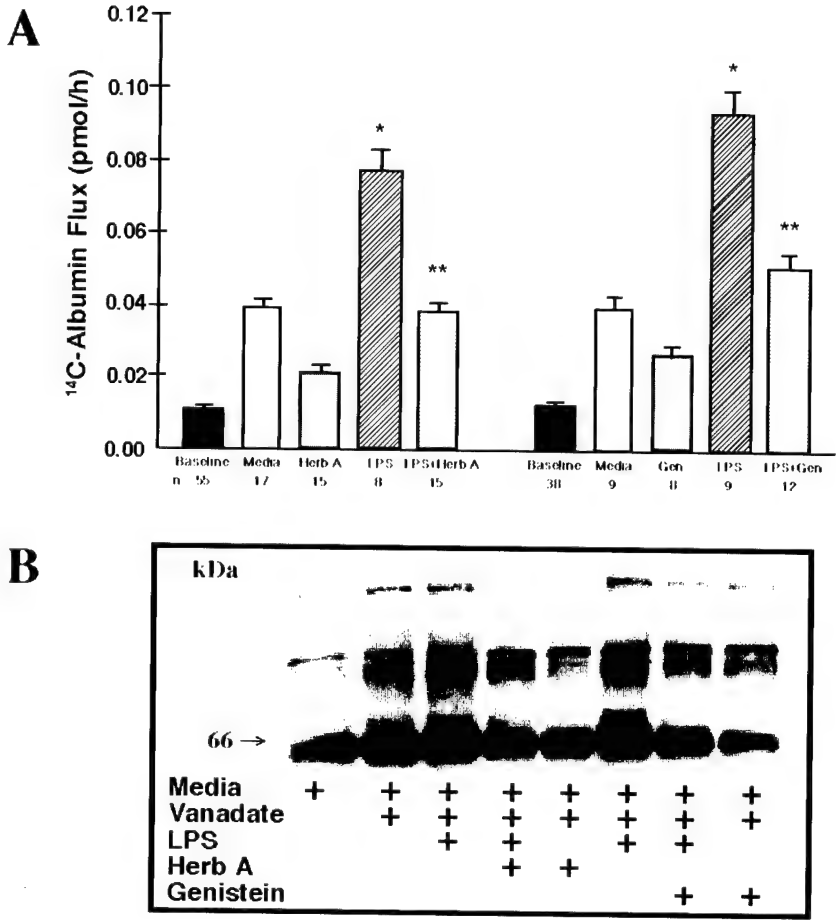
A
0.12
0.10
0.08
0.06
0.04
0.02
0.00
^{14}C-Albumin Flux (pmol/h)
*
**
*
**
Baseline
Media
Herb A
LPS
LPS+Herb A
Baseline
Media
Gen
LPS
LPS+Gen
n 35
17
15
8
15
38
9
8
9
12
B
kDa
66 →
Media + + + + + + + +
Vanadate + + + + + + +
LPS + + + + +
Herb A + +
Genistein + +

Figure 2

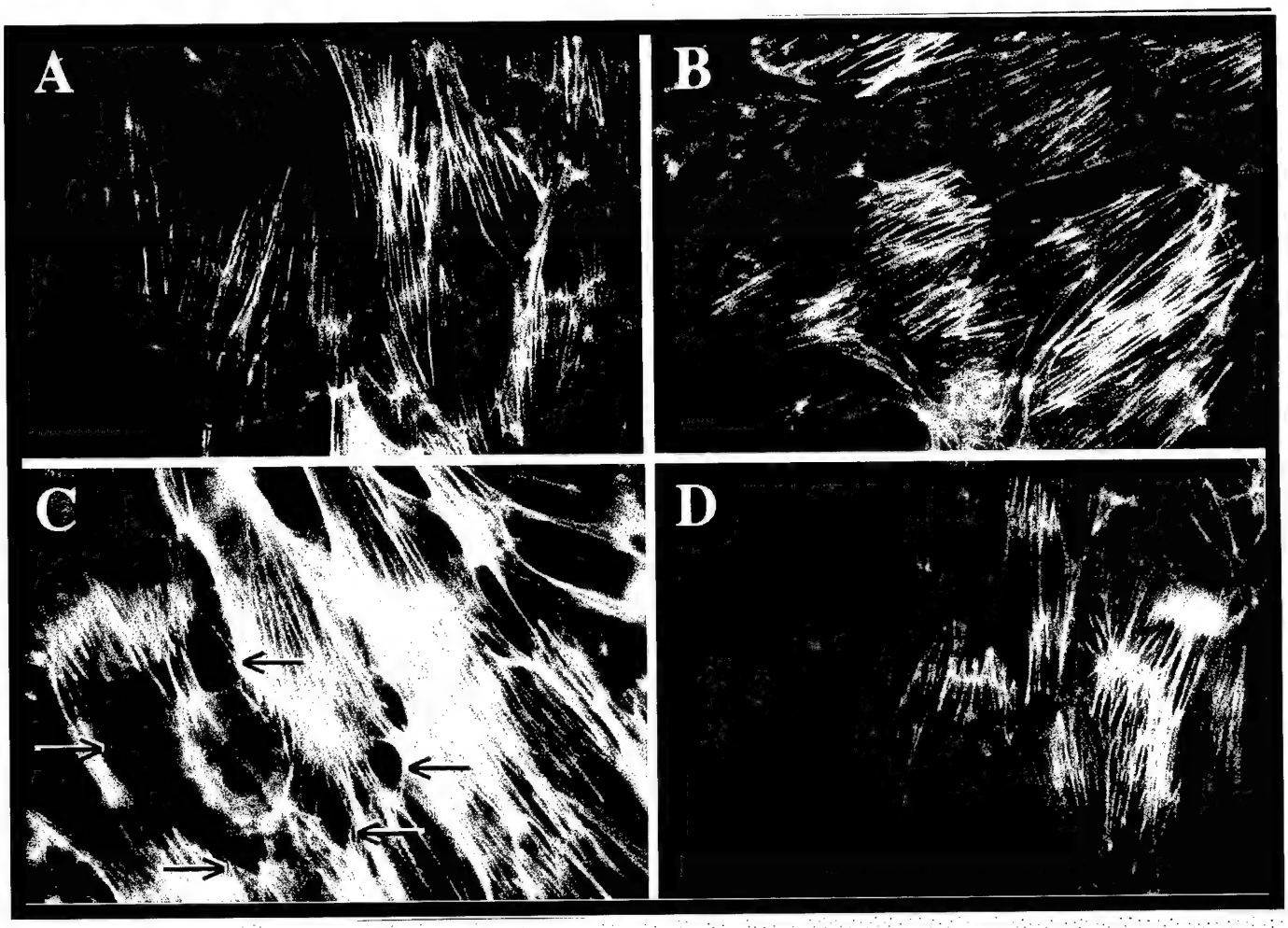

Figure 3

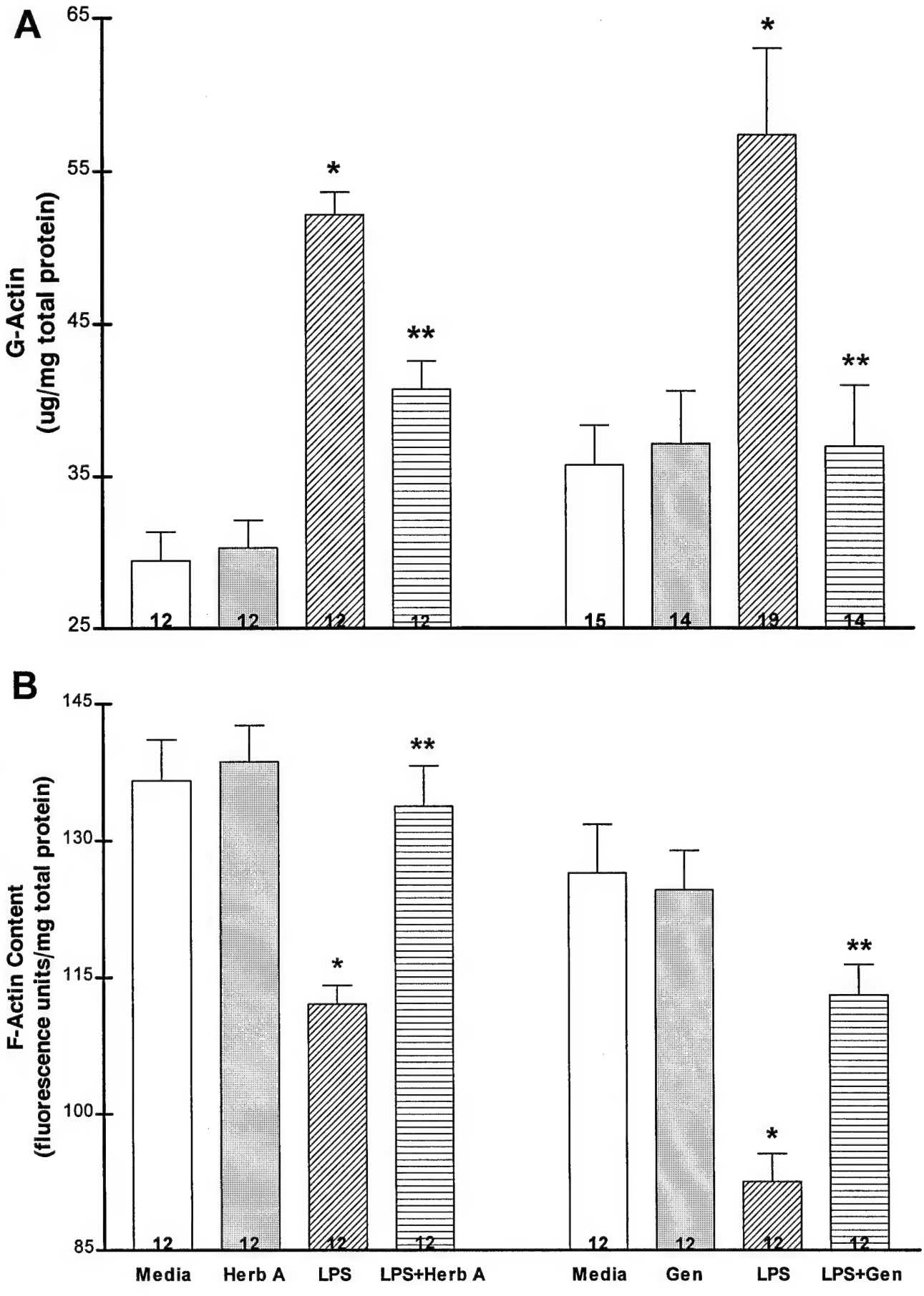
A
G-Actin
(ug/mg total protein)
65
55
45
35
25
12
12
12
12
15
14
19
14
*
**
*
**
B
F-Actin Content
(fluorescence units/mg total protein)
145
130
115
100
85
12
12
12
12
12
12
12
12
*
**
*
**
Media
Herb A
LPS
LPS+Herb A
Media
Gen
LPS
LPS+Gen

Figure 4

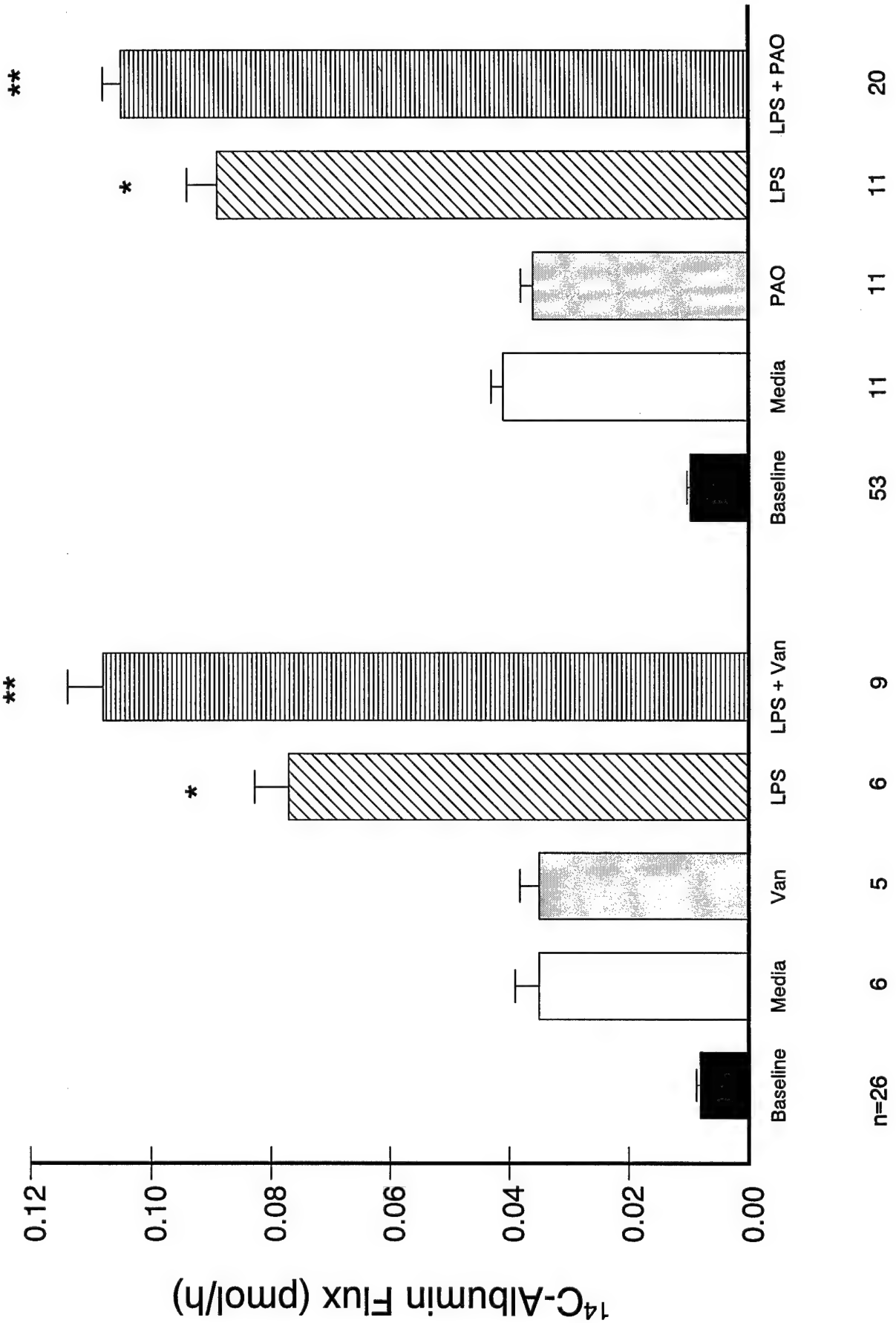
^{14}C-Albumin Flux (pmol/h)
0.12
0.10
0.08
0.06
0.04
0.02
0.00
**
*
*
**
Baseline
Media
Van
LPS
LPS + Van
Baseline
Media
PAO
LPS
LPS + PAO
n=26
6
5
6
9
53
11
11
11
20

Figure 5

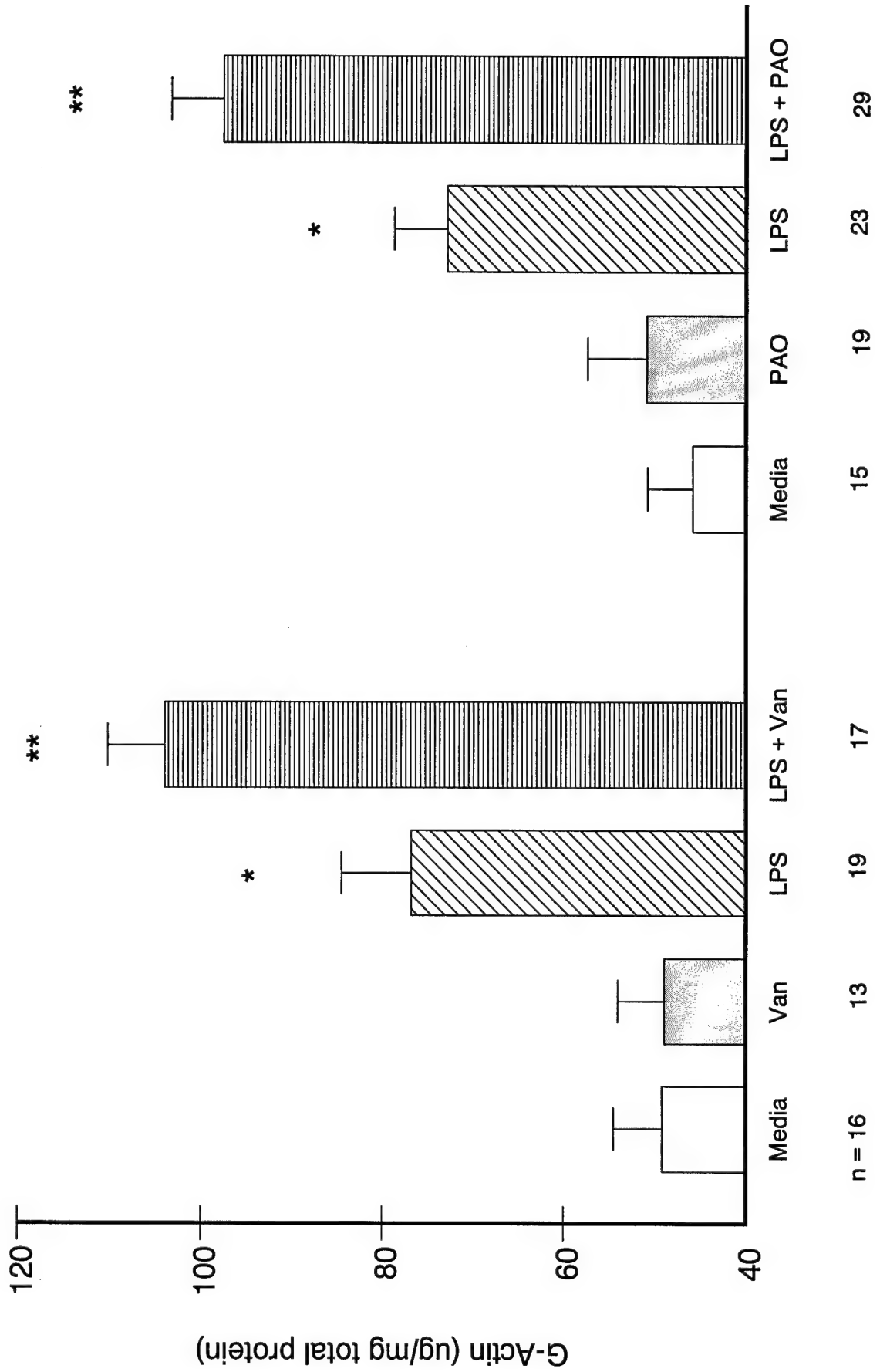
G-Actin (ug/mg total protein)
120
100
80
60
40
n = 16
13
19
17
15
19
23
29
Media
Van
LPS
LPS + Van
Media
PAO
LPS
LPS + PAO
*
**
*
**

Figure 6

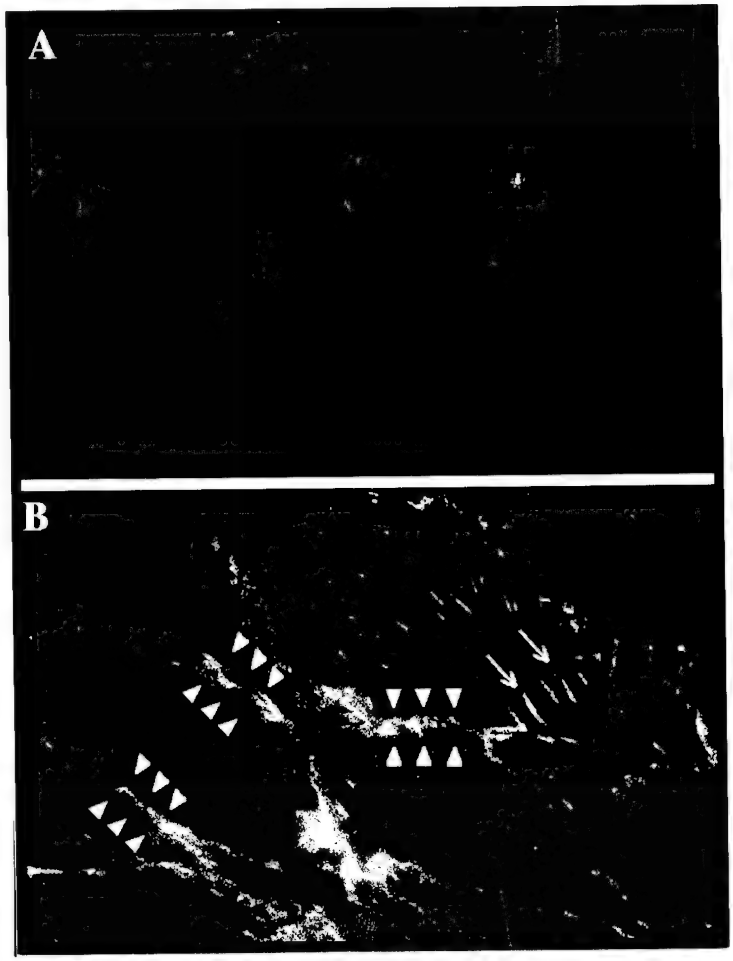

Figure 7

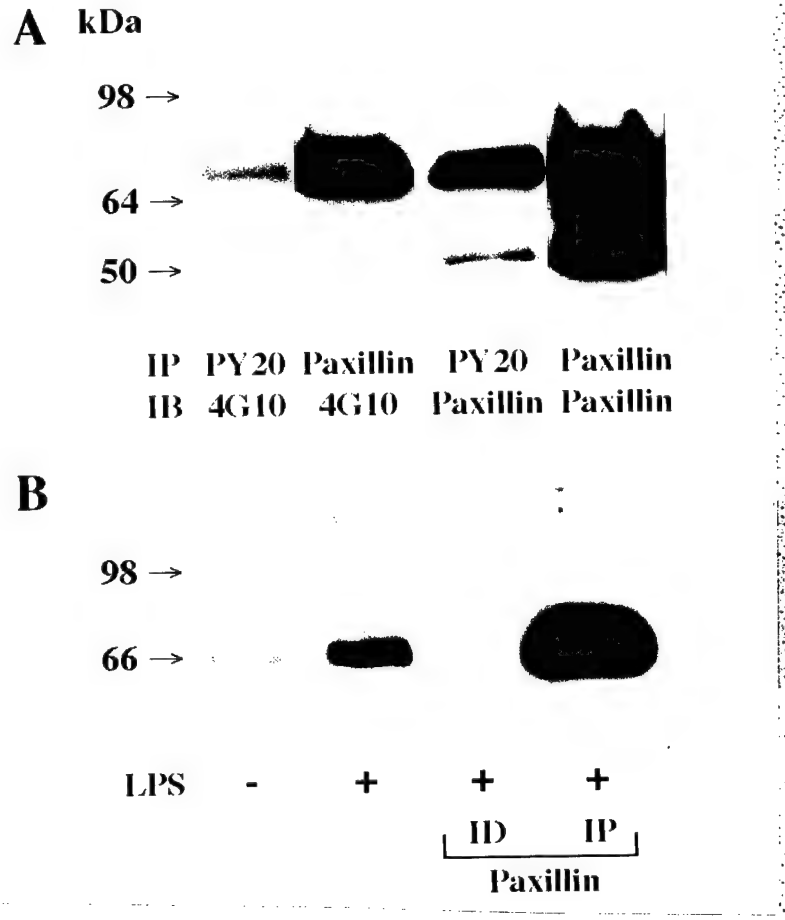
A
kDa
98 →
64 →
50 →
IP PY20 Paxillin PY20 Paxillin
IB 4G10 4G10 Paxillin Paxillin
B
98 →
66 →
LPS - + + +
IP
IB
Paxillin

Figure 8

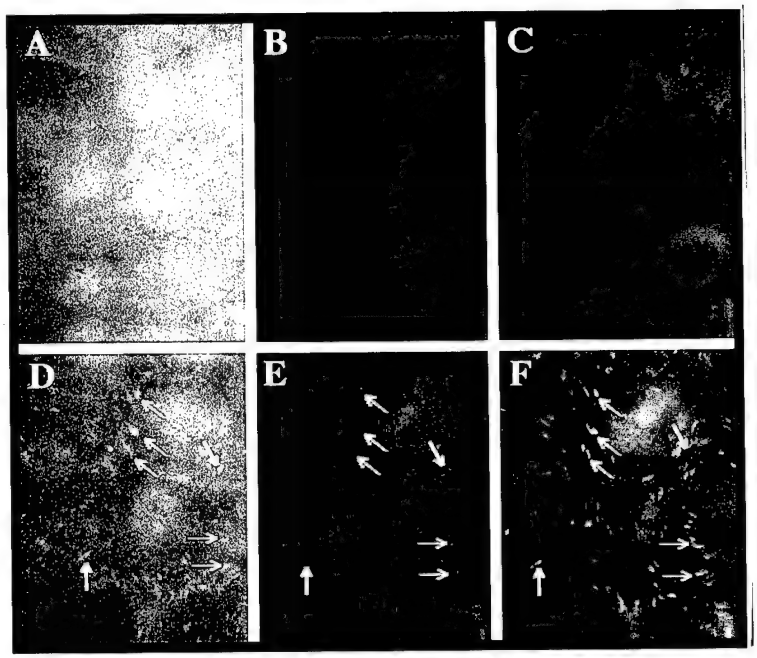

Figure 9

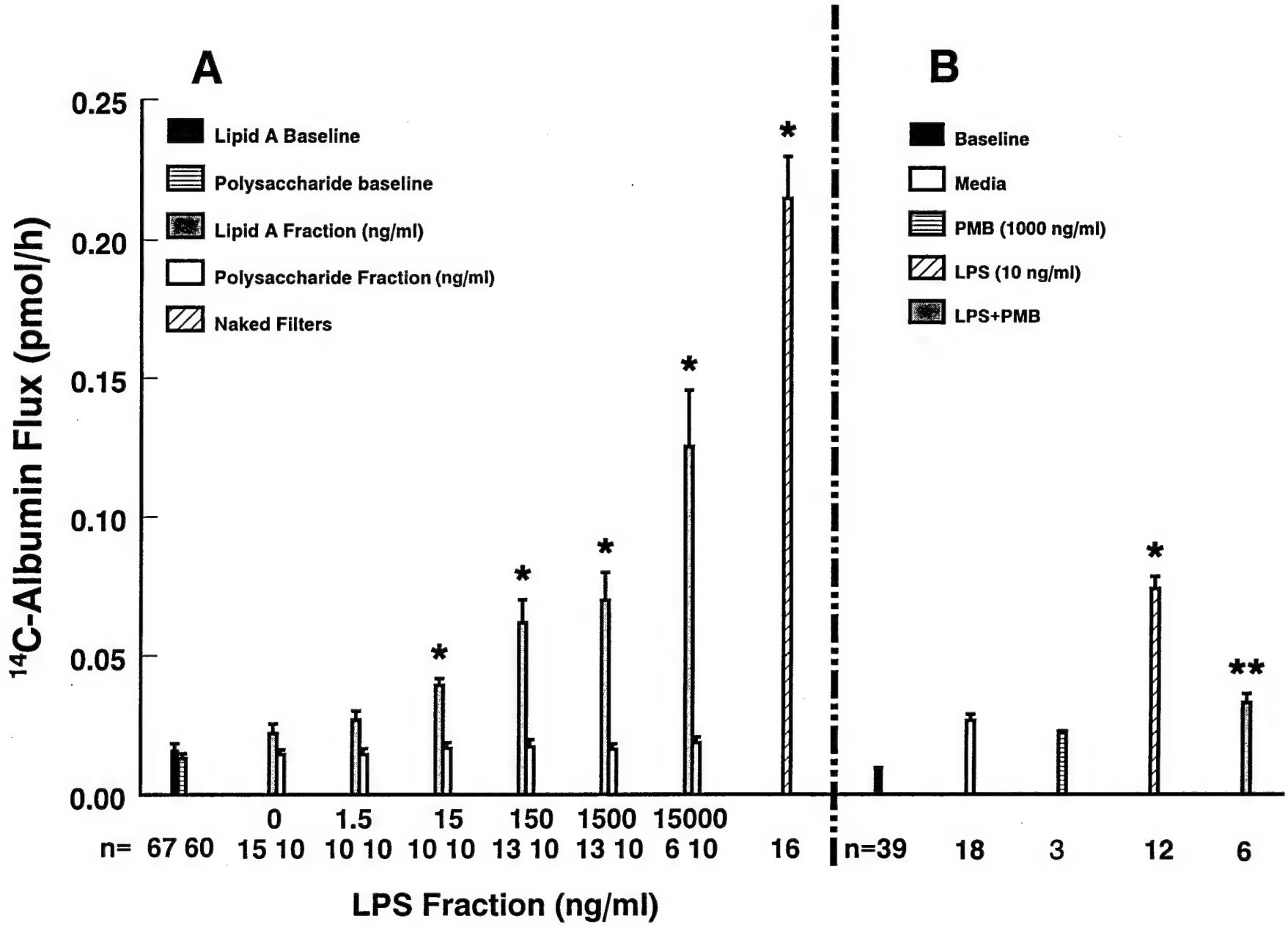
A
B
0.25
0.20
0.15
0.10
0.05
0.00
^{14}C-Albumin Flux (pmol/h)
Lipid A Baseline
Polysaccharide baseline
Lipid A Fraction (ng/ml)
Polysaccharide Fraction (ng/ml)
Naked Filters
Baseline
Media
PMB (1000 ng/ml)
LPS (10 ng/ml)
LPS+PMB
*
**
0
1.5
15
150
1500
15000
n= 67 60 15 10 10 10 10 10 13 10 13 10 6 10 16 n=39 18 3 12 6
LPS Fraction (ng/ml)

Figure 10

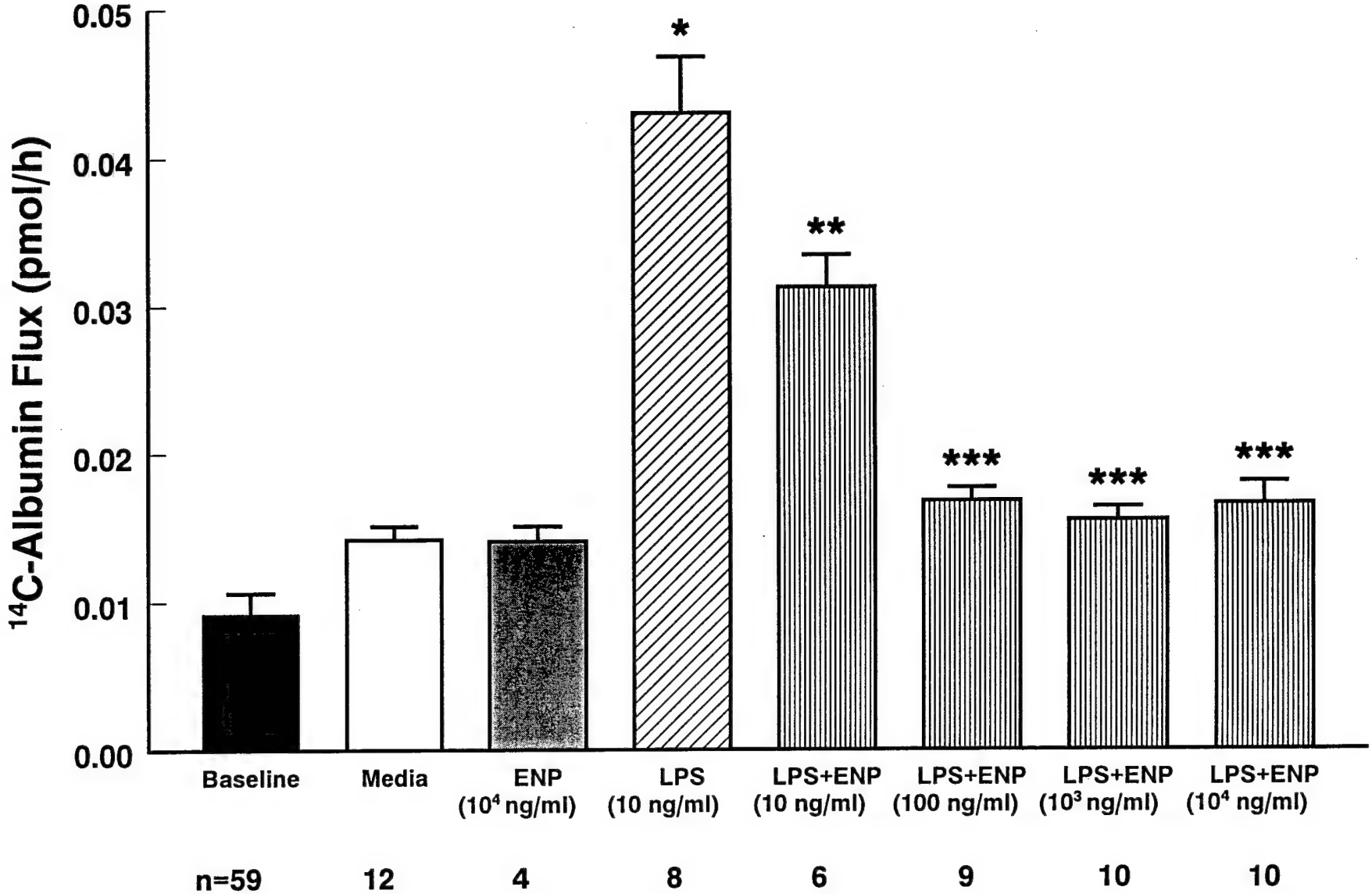
0.05
0.04
0.03
0.02
0.01
0.00
^{14}C-Albumin Flux (pmol/h)
*
**
***
***
***
Baseline
Media
ENP (10^4 ng/ml)
LPS (10 ng/ml)
LPS+ENP (10 ng/ml)
LPS+ENP (100 ng/ml)
LPS+ENP (10^3 ng/ml)
LPS+ENP (10^4 ng/ml)
n=59
12
4
8
6
9
10
10

Figure 11

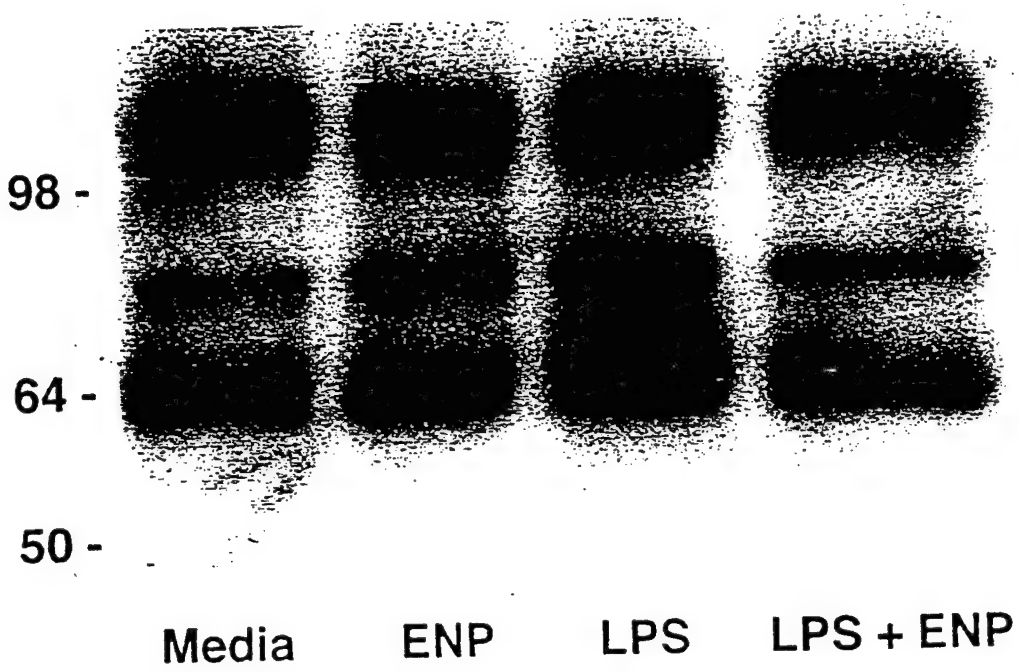

FIGURE 12

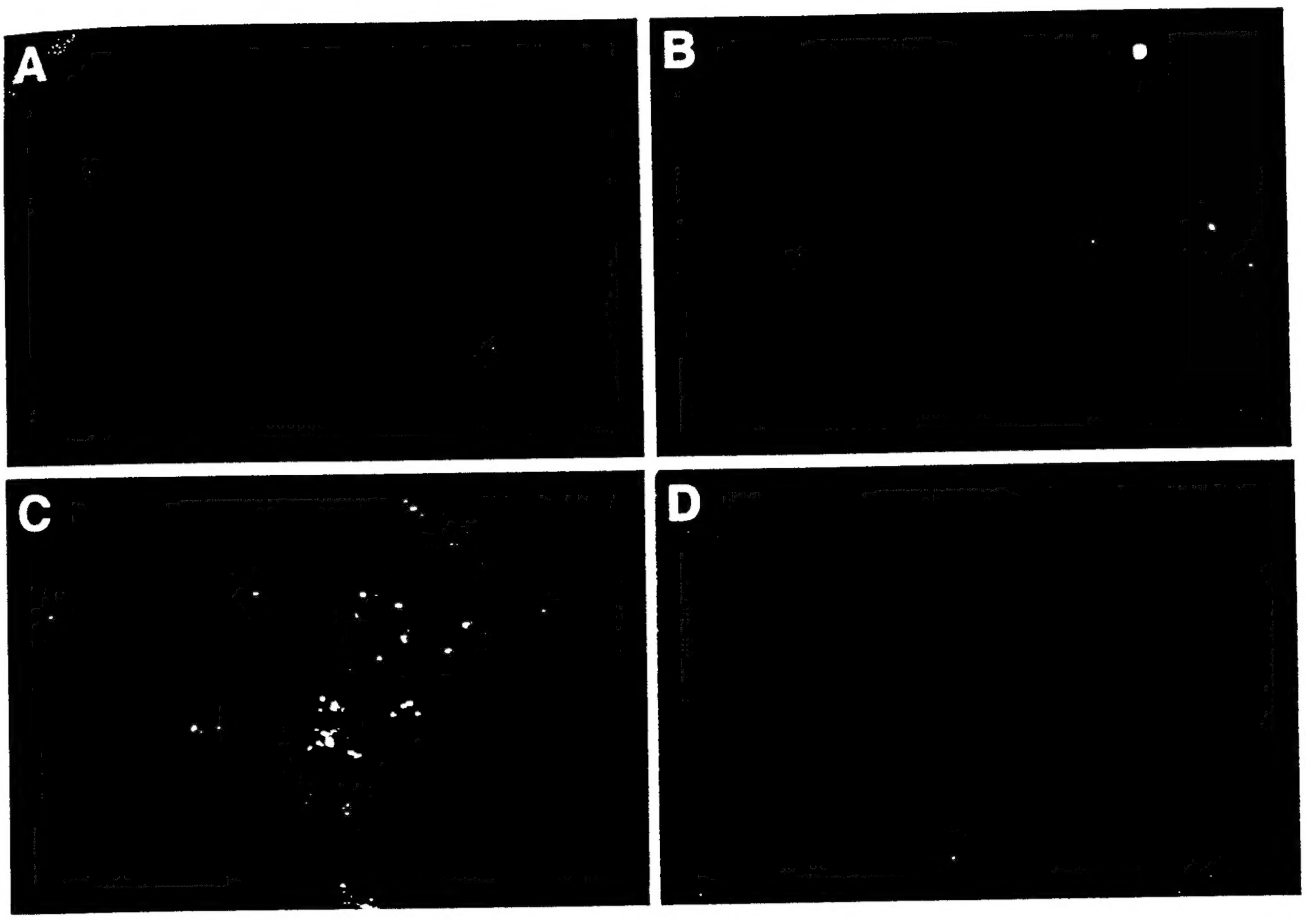

FIGURE 13

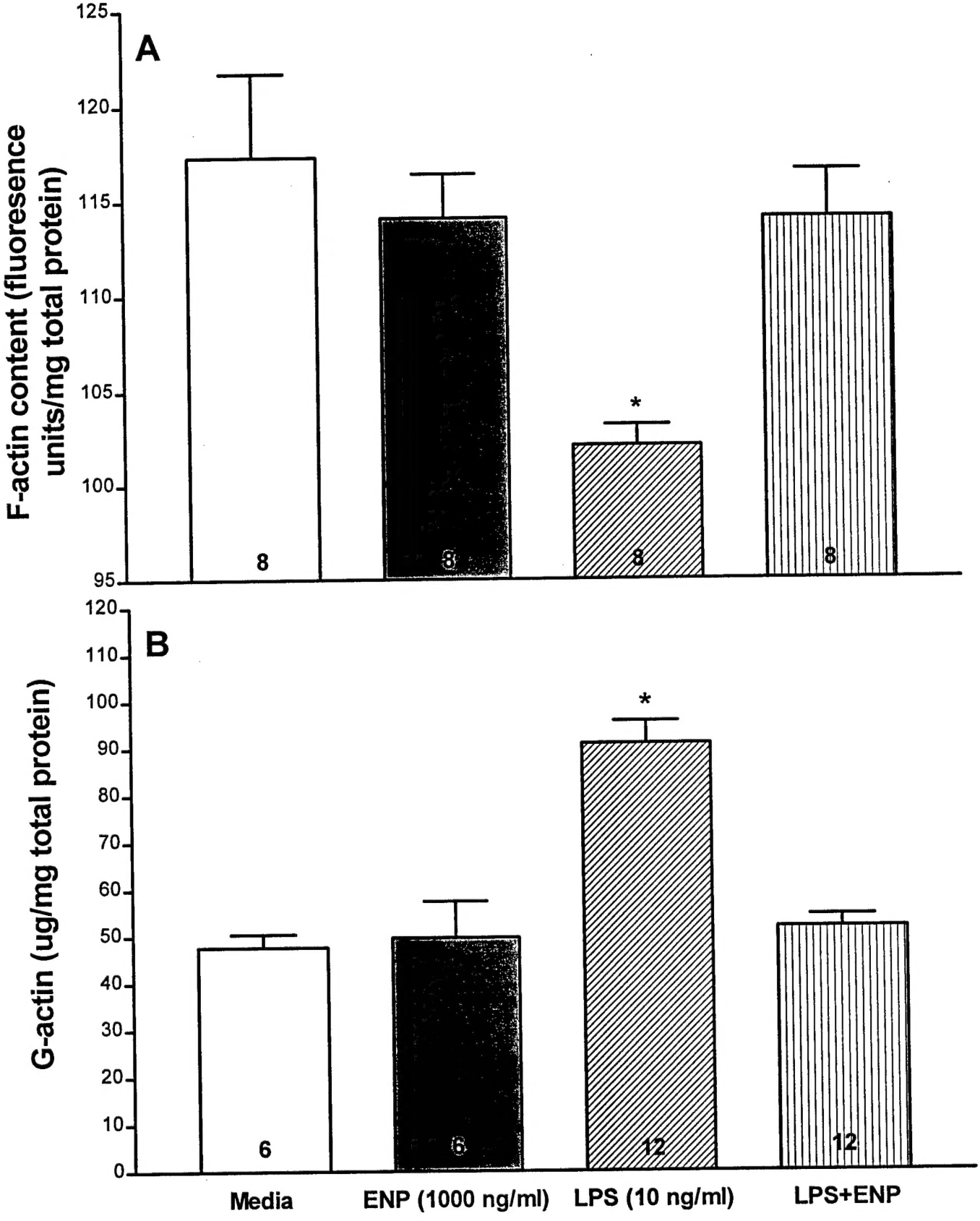
A
F-actin content (fluoresence units/mg total protein)
125
120
115
110
105
100
95
8
8
*
8
8
B
G-actin (ug/mg total protein)
120
110
100
90
80
70
60
50
40
30
20
10
0
6
6
*
12
12
Media
ENP (1000 ng/ml)
LPS (10 ng/ml)
LPS+ENP

Figure 14

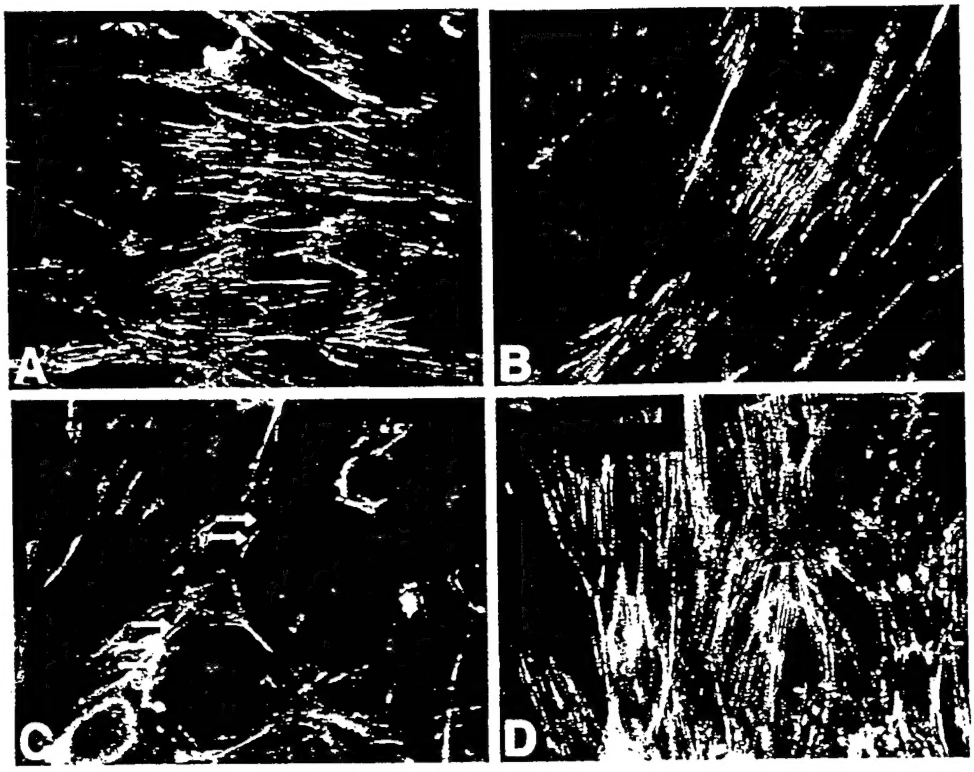

FIGURE 15

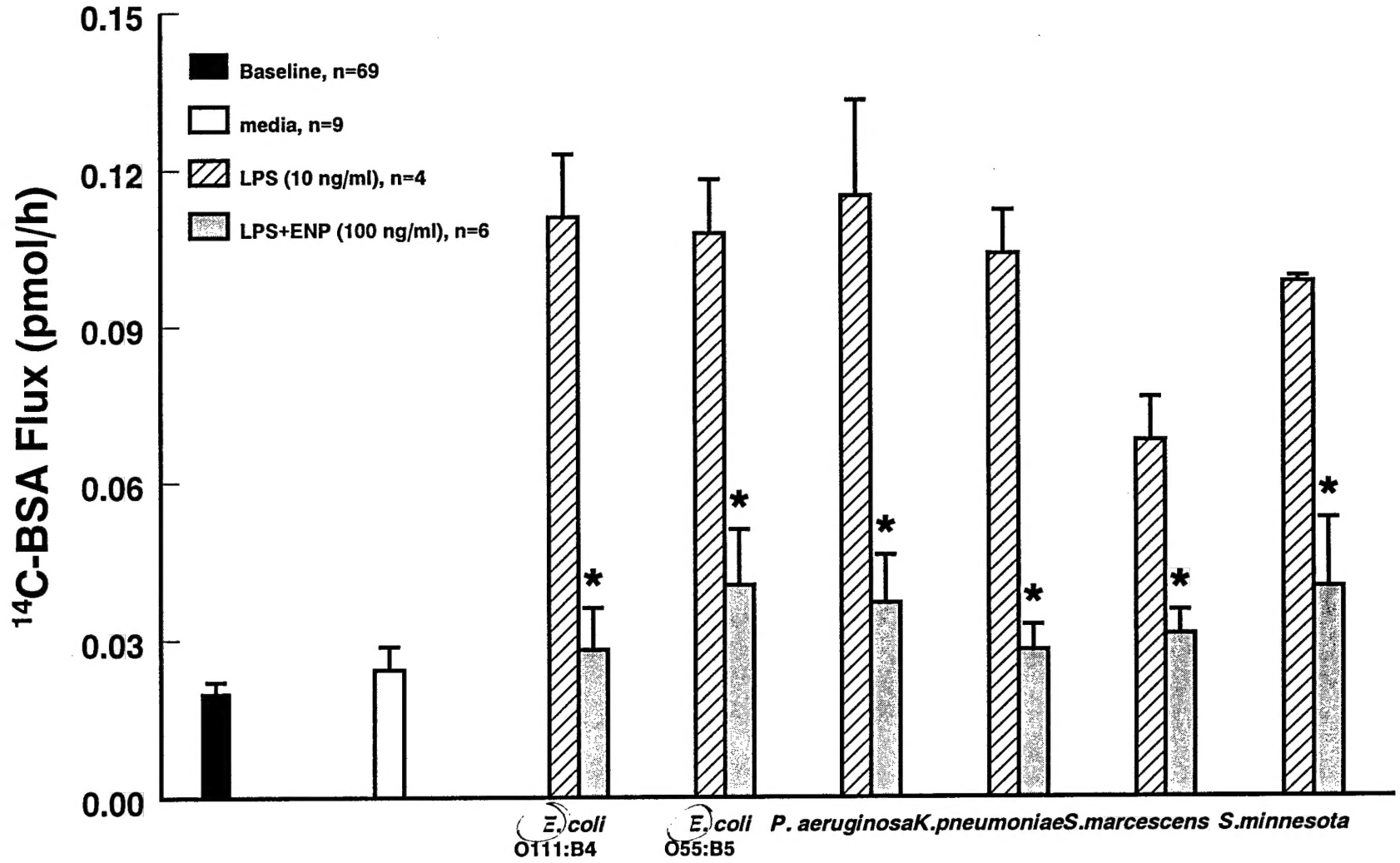
0.15
0.12
0.09
0.06
0.03
0.00
^{14}C-BSA Flux (pmol/h)
Baseline, n=69
media, n=9
LPS (10 ng/ml), n=4
LPS+ENP (100 ng/ml), n=6
*
E.coli O111:B4
E.coli O55:B5
P. aeruginosa
K.pneumoniae
S.marcescens
S.minnesota

Figure 16